



Strong influence of black carbon on aerosol optical properties in central Amazonia during the fire season

Rafael Stern¹, Joel F. de Brito², Samara Carbone³, Luciana Varanda Rizzo⁴, Jonathan Daniel Muller⁵, and Paulo Artaxo⁴

¹Climate and Environment Department, National Institute of Amazonia Research, Manaus, 69060-001, Brazil

²IMT Nord Europe, Institut Mines-Télécom, Université de Lille,
Centre for Energy and Environment, 59000, Lille, France

³Agrarian Sciences Institute, Federal University of Uberlândia, BR-050 – KM 78,
Uberlândia, 38410-337, Brazil

⁴Physics Institute, University of São Paulo, São Paulo, 05508-090, Brazil

⁵School for Climate Studies, Stellenbosch University, Stellenbosch 7600, South Africa

Correspondence: Rafael Stern (rafa.stern@yahoo.com.br)

Received: 26 October 2024 – Discussion started: 7 November 2024

Revised: 5 May 2025 – Accepted: 9 June 2025 – Published: 28 August 2025

Abstract. During the dry season, the Amazonian atmosphere is strongly impacted by fires, even in remote areas. However, there are still knowledge gaps regarding how each aerosol type affects the aerosol radiative forcing. This work characterizes the chemical composition of submicrometer aerosols and source apportionment of organic aerosols (OAs) and equivalent black carbon (eBC) to study their influence on light scattering and absorption at a remote site in central Amazonia during the dry season (August–December 2013). We applied positive matrix factorization (PMF) and multilinear regression (MLR) models to estimate chemical-dependent mass scattering efficiency (MSE) and extinction efficiency (MEE). Mean PM_1 aerosol mass loading was $6.3 \pm 3.3 \mu\text{g m}^{-3}$, with 77 % of organics, grouped into 3 factors: biomass burning OA (BBOA), isoprene-epoxydiol-derived secondary OA (IEPOX-SOA) and oxygenated OA (OOA). The bulk scattering and absorption coefficients at 637 nm were 17 ± 10 and $3 \pm 2 \text{ Mm}^{-1}$, yielding a single scattering albedo of 0.87 ± 0.03 . Although eBC represented only 6 % of the PM_1 mass loading, MSE was highest for the eBC ($13.58\text{--}7.62 \text{ m}^2 \text{ g}^{-1}$ at 450–700 nm), followed by BBOA ($7.96\text{--}3.10 \text{ m}^2 \text{ g}^{-1}$) and ammonium sulfate (AS, $4.79\text{--}4.58 \text{ m}^2 \text{ g}^{-1}$). The MEE was dominated by eBC (30.8 %), followed by OOA (19.9 %) and AS (17.6 %). The dominance of eBC over light scattering, in addition to absorption, plays a remarkably important role for this important climate agent, with potentially broad implications for more precise radiative forcing quantification, increasing climate modeling precision and representing deep contributions to Earth's climate system comprehension.

1 Introduction

The strong coupling between climate and the biological functioning of Amazonia is a key factor in the maintenance of its ecosystem (Martin et al., 2010b; Pöhlker et al., 2012). The Amazonian atmosphere is considered an important reactor, regulating its physical properties and chemical composition due to the high insolation and humidity (Andreae, 2001). However, during the dry season, forest fire emissions cou-

pled with smaller rates of aerosol scavenging lead to particle number concentration increases by a factor of 10 in remote forest areas compared with episodes of near pristine conditions during the wet season (Andreae et al., 2015; Artaxo et al., 2013; Pöhlker et al., 2018). These stark seasonal differences in aerosol loading and composition have the potential to significantly modify the biosphere–atmosphere coupling (Zaveri et al., 2022). These seasonal differences are expected

to be exacerbated in the future due to extreme climatic events in Amazonia (Flores et al., 2024).

Carbonaceous aerosols (i.e., organic aerosols (OAs) and black carbon (BC)) dominate the chemical classes of atmosphere particles in Amazonia (Artaxo et al., 2013). The secondary component of OA (SOA) has been shown to have a major contribution, notably during the wet season (Chen et al., 2015; Shrivastava et al., 2019). In remote regions of Amazonia, aged and highly processed oxygenated particles originating from multiple sources (forest fires, derived from volatile organic compounds (VOCs), etc.) are a major component of basin-wide haze observed during biomass burning season (Darbyshire et al., 2019). Isoprene (2-methyl-1, 3-butadiene, C₅H₈) is the most abundant VOC emitted globally, mostly in tropical forests (Marais et al., 2016; Yáñez-Serrano et al., 2015). The formation of isoprene-derived secondary organic aerosol (SOA) is a sequence of complex reactions and depends on different factors, such as low concentrations of NO and pre-existing aerosol particles on which isoprene can condense (Brito et al., 2018; Caravan et al., 2024; Marais et al., 2016; Nah et al., 2019). One of the dominating isoprene SOA pathways in Amazonia is through the OH attack, leading to hydroperoxy radicals (Shrivastava et al., 2019; Wennberg et al., 2018). This pathway can lead to different low-volatility products generally termed IEPOX-SOA (isoprene-epoxydiol-derived secondary organic aerosol) (Allan et al., 2014; Hu et al., 2015; Surratt et al., 2010). While OA originates from both primary emissions and secondary formation from gaseous precursors (Martin et al., 2010b), BC is mostly primarily emitted from incomplete combustion, and in remote areas of Amazonia it is associated with regional or transatlantic forest fires (Artaxo et al., 2013; Holanda et al., 2020; Saturno et al., 2018a). Atmospheric aerosol particles influence climate through scattering and absorption of solar radiation (aerosol–radiation interactions, ARIs) and by affecting cloud formation and lifetime (aerosol–cloud interactions, ACIs) (Forster et al., 2021). However, the magnitude and signal of global radiative forcing of aerosols still represent some of the largest uncertainties in global climate models (Szopa et al., 2023). Uncertainties on the radiative forcing of individual aerosol components are even higher, with a direct impact on the accuracy of future climate scenarios (Forster et al., 2021). The sign and magnitude of the ARI forcing are dependent on several parameters, such as particles' size distribution, mixture, aging processes, and meteorological conditions, as well as the particle chemical composition and its effect on the complex refractive index, based, among other factors, on the origin of the particles (Laskin et al., 2015; Li et al., 2024; Saturno et al., 2018a). Aerosol particles known for efficiently absorbing radiation – such as BC – often also exhibit significant scattering efficiencies, which are strongly influenced by their size, chemical composition, and the extent and nature of their atmospheric aging and coatings (Bond and Bergstrom, 2006; Schwarz et al., 2006; Yu et al., 2010). Although chemical aging has shown to en-

hance light absorption due to the coating of the BC core by condensing semi- and intermediate-volatility organic compounds or coagulation with other particles (Darbyshire et al., 2019; Metcalf et al., 2013; Saturno et al., 2018b; Tasoglu et al., 2017; Wang et al., 2016), primary biomass burning aerosols have also been associated with high scattering efficiencies (Hand and Malm, 2007; Malm et al., 2005). Coating by non-absorbing material, such as organics (Romshoo et al., 2021), has been shown to increase BC scattering by a factor of 3–24 depending on the size, morphology, aging stage, coating thickness, and composition of the BC particles (He et al., 2015). Conversely, sulfate and water coatings have also been shown to increase elemental carbon particle diameter, playing a stronger role in its scattering efficiency than absorption (Cheng et al., 2008; Yu et al., 2010). Precisely quantifying distinct ARIs for each chemical species, and especially reducing uncertainties on the ones with high potential to both absorb and scatter radiation, such as BC, is critical if we are to improve our understanding and prediction of the atmospheric system and improve climate models. Chemical composition, processes, and sources of atmospheric aerosol particles in Amazonia have been widely studied during both the wet and dry seasons, in sites representing pristine conditions (Andreae et al., 2015; Cheng et al., 2015; Martin et al., 2010a) as well as those strongly impacted by fires and urban pollution (Brito et al., 2014; Palm et al., 2018; Ponczek et al., 2021; Zaveri et al., 2022). Physical properties of radiation absorption and scattering have been described for the whole particles' mass loading, regardless of the specific chemical groups (Artaxo et al., 2013; Nascimento et al., 2021; Palacios et al., 2020; Rizzo et al., 2013; de Sá et al., 2019; Sena et al., 2013). However, intensive optical properties of each aerosol species are still rare (Velazquez-Garcia et al., 2023) and are notably associated with OA origins (Ponczek et al., 2021) and with BC behavior. Our study details the chemical properties of submicrometer aerosol particles in a forest site in central Amazonia during the dry season and their influence on radiation scattering and absorption. We applied positive matrix factorization (PMF) to the organic fraction and associated mass extinction, absorption, and scattering efficiencies to different aerosol components via multilinear regression (MLR) to improve our comprehension of their intrinsic properties and estimate their role in ARIs in central Amazonia during the dry season.

2 Material and methods

2.1 Sampling site

The measurement site is located in central Amazonia, 60 km northwest of the city of Manaus, Brazil, in the Cuieiras biological reserve (2°35'39.24'' S, 60°12'33.42'' W) (Martin et al., 2016; Whitehead et al., 2016). The vegetation is characterized as *terra firme* (upland forest, not impacted by seasonal flooding), and the canopy is between 30 and 35 m high

(Martin et al., 2010a). As a result of steady northeasterly–easterly winds (Andreae et al., 2015; Araújo et al., 2002), the site is only rarely impacted by Manaus' emissions (Chen et al., 2015). The wet season in this region is typically from 1 December–14 June and the dry season from 15 June–30 November (Andreae et al., 2015). During the wet season, air masses reaching the site pass over more than 1500 km of undisturbed forest (Pöschl et al., 2010). However, during the dry season, regional biomass burning pollution can be detected at the site (Artaxo et al., 2013; Rizzo et al., 2013) as well as aerosol plumes advected from African wildfires (Holanda et al., 2023). Our observations comprise readings taken from 1 August until 10 December 2013, sampling the atmosphere at 38.8 m above ground level. The instrumentation was located inside an air-conditioned container at the base of the tower. A cyclone (50 % cut-off at 10 µm) was used at the entrance of the inlet. An automatic diffusion dryer (Tuch et al., 2009) kept the relative humidity of the sampled air between 20 % and 50 %. Lodgings for scientists/staff and a diesel generator were located 330 and 720 m downwind (west) from the tower, respectively. The measurement tower has been shown to be practically unaffected by the generator (Whitehead et al., 2016). The year of this study (2013) was characterized by a historical minimum of fire detection over 20 years (Fig. 1; F. G. Assis et al., 2019), providing an interesting outlook to assess the best scenarios for a dry season in recent times and thus evaluate atmospheric composition within targets and goals for preservation of the Amazonia rainforest. The observation period here has been considered to fit entirely within dry-season atmospheric conditions. The previous transitional (wet-dry) period occurred in June–July (Whitehead et al., 2016), and the subsequent (dry-wet) one soon after the end of our measurements.

2.2 Instrumentation

Non-refractory submicrometer aerosol composition was measured using a quadrupole aerosol chemical speciation monitor (ACSM, Aerodyne Research Inc.) (Ng et al., 2011), which is a compact version of the aerosol mass spectrometer (AMS). Instrument calibration consisted of injecting monodispersed (300 nm) aerosol particles of ammonium nitrate (AN) and ammonium sulfate (AS), generated using an atomizer and subsequently dried, with the size selected using a differential mobility analyzer. A collection efficiency of 0.5 was adopted (Middlebrook et al., 2012), yielding a very good agreement of particle mass considering measurements from different collocated instruments (S1). This method was successfully used in previous studies (Brito et al., 2014; Sun et al., 2010), and the value of 0.5 agrees with other studies in Amazonia during the dry season (Ponczek et al., 2021; de Sá et al., 2019). The measured ammonium (NH_4) mass concentrations were close to, or often lower than, the detection limit of $0.28 \mu\text{g m}^{-3}$ (Pöhlker et al., 2018; Whitehead et al., 2016) and were therefore calculated based on nitrate (NO_3^-)

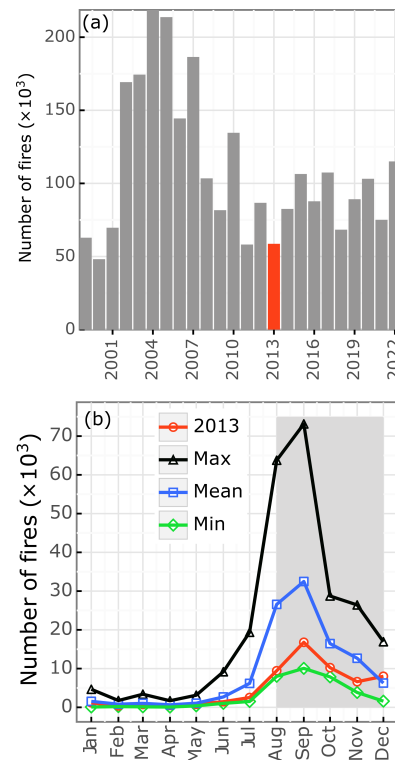


Figure 1. (a) Number of fires in the Brazilian Amazonia rainforest from 1999 to 2022, showing how 2013 (marked in red) has the lowest total number of fires in 20 years, and (b) mean (blue), maximum (black), and minimum (green) monthly fires between 1999–2022 in the Amazonian Basin. The year of 2013 is marked in red, and it is evident how it was very close to the minimum (green) line. The gray area in panel (b) marks the period of measurements in our study (1 August–10 December) (Instituto Nacional de Pesquisas Espaciais, 2024).

and sulfate (SO_4^{2-}) molar masses and their mass concentrations, assuming neutralization as in Eq. (1).

$$\text{NH}_4, \text{predicted} = 18 \times \left(\frac{\text{SO}_4}{96} \times 2 + \frac{\text{NO}_3}{62} \right) \quad (1)$$

Furthermore, the SO_4^{2-} and NO_3^- ions were used to estimate AS and AN (Eqs. 2 and 3) for the chemical-dependent optical properties analyses (Sect. 3.3), assumed here to be their most abundant form given the very low NH_4^+ levels.

$$\text{AS} = 132 \times \frac{\text{SO}_4}{96} \quad (2)$$

$$\text{AN} = 80 \times \frac{\text{NO}_3}{62} \quad (3)$$

Size-resolved particle number size distribution from 10 to 450 nm was measured with a scanning mobility particle sizer (SMPS, model 3081, TSI Inc.) coupled to a condensation particle counter (CPC, model 3772, TSI Inc.) to provide equivalent mobility particle diameters for singly charged particles (D_{pg} , Wiedensohler et al., 2012). The aerosol light

scattering coefficient (σ_s) at 450, 550, and 700 nm (Anderson and Ogren, 1998) was measured using a nephelometer (model 3563, TSI Inc.). Calibration was performed using CO₂ as the high-span gas and filtered air as the low-span gas. The averaging time applied was 60 min, and therefore the detection limits (defined as a signal-to-noise ratio of 2) for scattering coefficients were 0.08, 0.03, and 0.05 Mm⁻¹ for 450, 550, and 700 nm, respectively (Anderson and Ogren, 1998). Since a PM₁₀ inlet was used, the “no-cut” factors were used for the truncation corrections. We used a multi-angle absorption photometer (MAAP, model 5012, Thermo Electron Group, Waltham, USA) (Müller et al., 2011) to measure the aerosol light absorption coefficient (σ_a) at 637 nm and to estimate equivalent black carbon (eBC) concentration, assuming an absorption cross-section value of 6.6 m² g⁻¹. Considering the conditions of the experiment, the MAAP detection limit for σ_a was of 0.13 Mm⁻¹ (Petzold et al., 2005).

Episodes of possible contamination from the city of Manaus and from the diesel generator were removed by filtering the data points when either the wind direction was 270–340° (from our local wind direction measurements) or when the calculated back-trajectories from the HYSPLIT model (Draxler and Hess, 1998) passed over Manaus' coordinates, as in (Whitehead et al., 2016) (Sect. S2 in the Supplement).

2.3 Optical properties

Scattering coefficients at 637 nm were calculated from interpolation using the scattering Ångström exponent (α_s , Eq. 4), assuming a power-law spectral dependency. The α_s is a measure of the dependence of radiation scattering on the light wavelength (λ) and is an indication of particle size (Rizzo et al., 2013; Saturno et al., 2018b; Schuster et al., 2006).

$$\ln \sigma_s = -\alpha_s \ln \lambda + \ln(\text{constant}) \quad (4)$$

Single scattering albedo (SSA, Eq. 5) is a measure of the ratio of σ_s to the total radiation extinction coefficient ($\sigma_e = \sigma_s + \sigma_a$) by aerosol particles (Rizzo et al., 2013). Since the MAAP instrument only measures σ_a at a wavelength of 637 nm, σ_e was calculated using σ_s at 637 nm interpolated from the nephelometer.

$$\text{SSA} = \frac{\sigma_s}{\sigma_s + \sigma_a} \quad (5)$$

After rain events and other moments when the atmosphere is very clean, all the optical parameters are close to zero, and therefore the ratio between them becomes unrealistically high. We therefore calculated SSA only when σ_s and $\sigma_e > 1 \text{ Mm}^{-1}$.

2.4 Statistical analyses

2.4.1 Positive matrix factorization (PMF)

We used positive matrix factorization (PMF) in order to group the submicrometer non-refractory organic mass spec-

tra (m/z ratios) with similar temporal variability, supporting the identification of sources and processes that formed and transformed atmospheric particles (Paatero and Tapper, 1994; Ulbrich et al., 2009; Zhang et al., 2011). The model can be represented by Eq. (6),

$$\mathbf{X}_{(m \times n)} = \sum \mathbf{G}_{(m \times p)} \mathbf{F}_{(p \times n)} + E, \quad (6)$$

where \mathbf{X} is the input matrix of n (elements – m/z ratios) lines and m (number of samples) columns (Ulbrich et al., 2009). In this study, the \mathbf{X} matrix had 2901 lines (1 h averages for more than 4 months of measurements) and 70 columns (m/z ratios). The receptor model aims to determine the number of p factors, representing sources or processes, their chemical composition, and the relative contribution of each factor. In matrix \mathbf{G} , the columns are the time series of the factors. In matrix \mathbf{F} , the lines are the profiles of the factors (mass spectra). The residuals E are the part of the data that was not modeled by any factor p . We used an IGOR™-based interface to apply the PMF analysis (Ulbrich et al., 2009). The PMF ions were normalized to the organics concentration.

2.4.2 Multilinear regression (MLR)

We used a multilinear regression (MLR) model to estimate the contribution of each aerosol chemical component to scattering, absorption, and extinction coefficients, deriving the corresponding efficiencies (mass scattering efficiency, MSE; mass absorption efficiency, MAE; and mass extinction efficiency, MEE; respectively) (Yu et al., 2010). The scattering (σ_s) and extinction (σ_e) coefficients (Mm⁻¹) were the dependent variables (response), and the ACSM species/PMF factors were the independent (predictor) variables.

A generalization of the mass efficiency (ME) calculation is presented in Eq. (7),

$$\text{ME} = \sum_i a_i x_i + r, \quad (7)$$

where ME can be MSE, MAE, or MEE, x is the chemical species mass concentration, a_i is the efficiency of each component, and r represents the residuals. We used NNLS (non-negative least squares) from the Python package SciPy version 1.5.2 (Virtanen et al., 2020). To constrain the model to produce results with physical meaning, the coefficients a_i were constrained to be positive, as in Velazquez-Garcia et al. (2023). Since eBC is assumed to be the only absorbing component measured in this study with the MAAP, an MLR could not be applied for σ_a , and the MAE was considered to be equivalent to the cross-section value (6.6 m⁻² g⁻¹, Sect. 2.2).

3 Results and discussion

3.1 Aerosol chemical composition

The concentrations of organics and inorganics aerosols follow similar variation patterns during the measurement period (Fig. 2a). This can be an indication that the total mass loading consists of well-mixed biomass burning and secondary aerosols associated with large and regional-scale processes (Darbyshire et al., 2019). The total submicrometer ($\text{PM}_1 = \text{Organics} + \text{NO}_3 + \text{NH}_4 + \text{SO}_4 + \text{eBC}$) mean mass concentration during the observation period was $6.3 \pm 3.3 \mu\text{g m}^{-3}$ (Table 1, Fig. 2a). This represents about half of what was measured during the dry season of the following year (2014, with many more fires; see Fig. 1) at a nearby site with similar conditions in central Amazonia (ATTO, de Sá et al., 2019) and regions directly impacted by fires during the dry season (Brito et al., 2014; Ponczek et al., 2021). The PM_1 aerosol composition was dominated by the organic fraction ($77 \pm 5 \%$, Table 1, Fig. 2b), similar to what was found in the same site in wetter conditions (Artaxo et al., 2013; Chen et al., 2015; Whitehead et al., 2016) but lower than what was found in a region highly impacted by biomass burning in southwestern Amazonia (Brito et al., 2014). In continental urban areas, such as across Europe, the organic particles represented a much lower fraction of the total particle mass (Chen et al., 2022). Sulfate is the main soluble inorganic component of the aerosol mass fraction in Amazonia, during both the wet and dry seasons (Fuzzi et al., 2007; Yamasoe et al., 2000). In our study, the mean SO_4 mass fraction was $9 \pm 3 \%$ (Table 1, Fig. 2b), which is comparable to the ATTO site (Andreae et al., 2015). However, in southwestern Amazonia, in areas impacted by fresh biomass burning, the average SO_4 mass fraction was significantly lower (2–3 %; Brito et al., 2014; Ponczek et al., 2021).

The eBC mass fraction was $6 \pm 2 \%$ (Table 1, Fig. 2b), which is half of the fraction observed in the wet season at the same site (Chen et al., 2015), despite the much lower total submicrometer aerosol mass loading. Occasional urban pollution from Manaus, long-range transport from Africa, and potential artifacts combined with much lower overall aerosol loading are possible causes for this higher eBC mass fraction found in the wet season (Chen et al., 2015). In southwestern Amazonia, highly impacted by fresh biomass burning, the contribution of eBC to PM_1 reached 15 % (Ponczek et al., 2021). Nitrate had a minor contribution during our observations ($3 \pm 1 \%$), with concentration levels comparable to the ATTO site (Pöhlker et al., 2018) as well as southwestern Amazonia (Brito et al., 2014; Ponczek et al., 2021).

The PMF analysis yielded 4 statistical factors, although 2 of them were closely related to the oxygenated organic aerosol (OOA) fraction. The mass spectra, daily profile, and time series of these factors did not present enough differences to justify their separation (Sects. S3 and S4). Therefore, these 2 factors were manually summed in order to generate a 3-

Table 1. Dry season (1 August–10 December) mean mass concentration (μm^{-3}), standard deviations, and percentile range (10–90, in parenthesis) of the species measured by the ACSM and MAAP (eBC).

	Mass concentration ($\mu\text{g m}^{-3}$)	Mass fraction
Total PM_1	6.3 ± 3.3 (2.7–10.3)	100 %
Organics	4.9 ± 2.7 (2.1–7.9)	$77 \pm 5 \%$
BBOA	0.6 ± 0.6 (0.2–1.1)	$9 \pm 5 \%$
IEPOX-SOA	1.0 ± 0.5 (0.4–1.7)	$17 \pm 5 \%$
OOA	3.2 ± 1.5 (1.3–5.5)	$51 \pm 6 \%$
NO_3	0.2 ± 0.1 (0.1–0.3)	$3 \pm 1 \%$
NH_4	0.3 ± 0.1 (0.0–0.5)	$4 \pm 1 \%$
SO_4	0.5 ± 0.3 (0.2–0.9)	$9 \pm 3 \%$
eBC	0.4 ± 0.3 (0.1–0.7)	$6 \pm 2 \%$

factor solution, which was different from the factors found in the 3-factor solution presented by the PMF. In Ulbrich et al. (2009), the authors describe how one PMF resulting statistical factor can split into various other factors which, after being added, represent the real factor. The recombination often considers similarities between the statistical factors in the mass spectra, daily profile, and time series (Carbone et al., 2013). In our study, the identification of the factors was further confirmed with the correlation between the PMF statistical factors and the inorganic aerosols with the eBC (Sect. S4) and daily profile analyses. The 3 factors were identified as BBOA (biomass burning organic aerosol), OOA (oxygenated organic aerosol), and IEPOX-SOA (isoprene-epoxydiol-derived secondary organic aerosol), and together they represent 99 % of the measured submicrometer organic aerosol mass, with 1 % of residuals. The correlation between BBOA and NO_3 and SO_4 is comparable with findings in southwestern Amazonia (Brito et al., 2014). The dominant PMF-derived statistical factor in our study was OOA, which contributed to $51 \pm 6 \%$ of the PM_1 (Table 1) and 65 % of the organic mass. This agrees with previous studies showing that highly processed SOAs are a major component of the atmospheric particles in remote regions of Amazonia (Darbyshire et al., 2019). This factor has the highest estimated O:C ratio, which is evident in the observed m/z 44 fraction (Fig. 3; note the different scales). The high oxidation level indicates highly aged particles, and they may lose some of their original chemical signatures, in terms of elementary ratios, during the aging process (Jimenez et al., 2009). The m/z 44 signal predominantly arises from the CO_2^+ ion fragment, which is typically generated by thermal decarboxylation of carboxylic acid functional groups in organic aerosols (Alfarra et al., 2004). Therefore, m/z 44 serves as a valuable marker for the

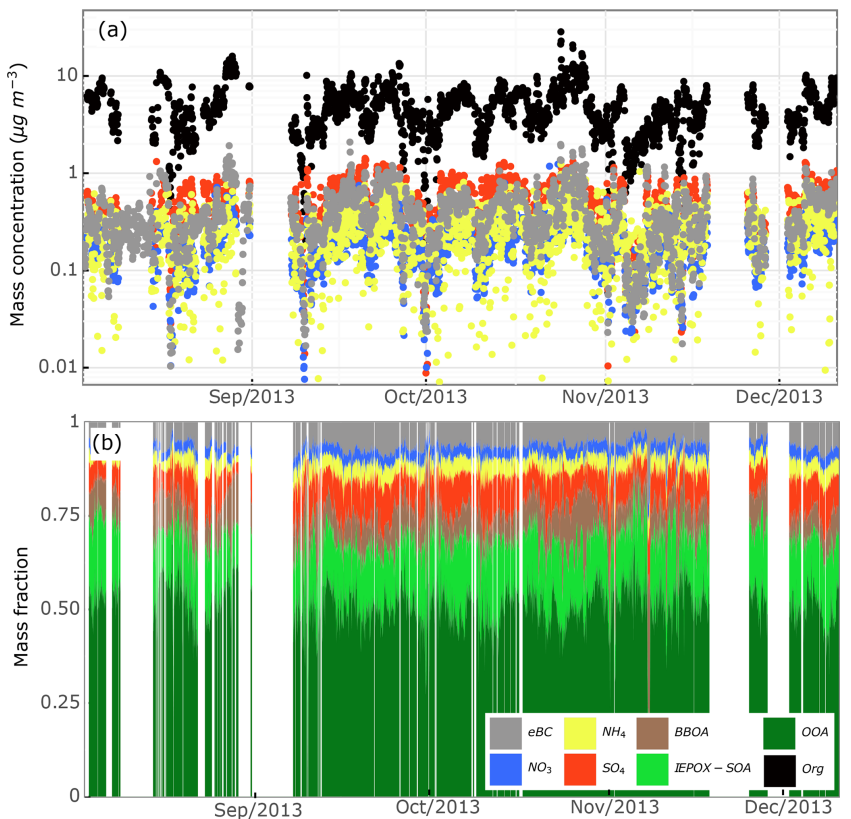


Figure 2. Non-refractory submicrometer aerosol species and eBC mass **(a)** concentrations and **(b)** fractions. In panel **(a)**, the vertical axis is the logarithm scale to facilitate the visualization of different species.

extent of aerosol oxidation and the presence of oxygenated organic compounds, providing insight into aerosol aging and secondary organic aerosol formation processes. The more aged the aerosols, the more chemically similar they become, which makes the task of separating them into different factors with distinctive characteristics very difficult. Therefore, the OOA factor probably groups aerosol particles from different sources, and their common characteristic is that they probably originate relatively distant from the sampling site.

The production of IEPOX-SOA generally leads to the production of markers in the atmosphere, such as the 2-methyltetrols and the 3-methylfuran (m/z 82, $\text{C}_5\text{H}_6\text{O}^+$) (Lin et al., 2012). The organic fraction in the m/z 82 is therefore important for the identification of the IEPOX-SOA factor (Fig. 3b), despite its low contribution to the mass fraction (usually below 4 % of submicrometer organic aerosol). Most of the other m/z are common to other factors, making the m/z 82 distinctive of the IEPOX-SOA, which can also be identified by the m/z 53 (C_4H_5^+) and m/z 75 ($\text{C}_3\text{H}_7\text{O}_2^+$) (Fig. 3b) (Allan et al., 2004; Lin et al., 2012; Xu et al., 2015). The IEPOX-SOA mean mass concentration in our study was $1.0 \pm 0.5 \mu\text{g m}^{-3}$ (Table 1). Previous studies reported $0.26 \mu\text{g m}^{-3}$ during the wet season at the same site (Chen et al., 2015), while downwind of Manaus it was around

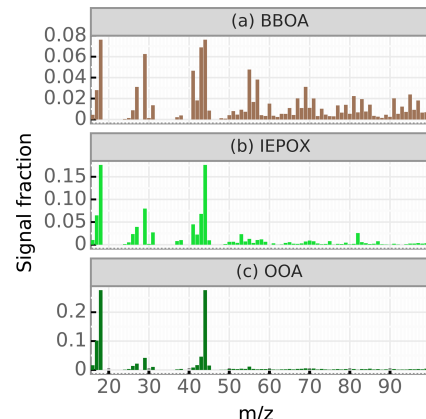


Figure 3. PMF mass spectra composition of each statistical factor and its relative contribution to the total submicrometer organic aerosol mass. It is possible to observe typical tracer ions such as m/z 60 and m/z 73 that characterize the BBOA factor and also m/z 82 in the IEPOX-SOA factor. The scale of the y axis is different in order to facilitate visualization of m/z signal fractions mainly of panels **(a)** and **(b)**.

$0.5 \mu\text{g m}^{-3}$ during background conditions and $0.1 \mu\text{g m}^{-3}$ during polluted conditions (de Sá et al., 2017).

While the organic particle loading typically increases by an order of magnitude from the wet to the dry season (Artaxo et al., 2013), IEPOX-SOA increases by a factor of about ~ 3 (Table 1 and Chen et al., 2015), while its relative contribution to the organic aerosols drops by half (from 34 % (Chen et al., 2015) to 17%; Table 1). This is likely the result of a complex balance between increased isoprene emissions (Yáñez-Serrano et al., 2015), sulfate abundance, and increased pollution levels (including NO_x from forest fires and biomass-burning-related aerosol particles). The relative contribution of IEPOX-SOA to the total PM_{1} mass was relatively constant during the whole measurement period (Fig. 2b), as well as most of the other species (with the exception of some episodes). This indicates that an atmospheric dynamics of rain/dilution controlling the chemical composition could be more important than the influence of local sources of particles, confirming the regional haze hypothesis raised by Darbyshire et al. (2019).

The correlation (Pearson coefficient = 0.7) observed between the IEPOX-SOA factor and AS (Fig. S11) is similar to the correlation measured in regions affected by urban pollution in Amazonia, Africa, and the USA (Brito et al., 2018; Budisulistiorini et al., 2013; de Sá et al., 2017). Sulfate is the main aqueous phase particle on which isoprene products condense, and therefore a positive and moderate-high correlation is expected (Budisulistiorini et al., 2013; Kroll et al., 2006; Lin et al., 2012; Marais et al., 2016; Surratt et al., 2010; Xu et al., 2015). eBC presents a similar correlation with IEPOX-SOA as AS (Sect. S4), but the correlation is even higher with the other PMF factors, especially OOA (Pearson coefficient = 0.85, Sect. S4). This suggests that a significant fraction of the aged submicrometer aerosols measured during the dry season in central Amazonia is largely influenced by biomass burning emissions, in combination with other combustion sources such as sporadic urban plumes transported from Manaus. In addition, co-variability between aerosol species is expected due to strong washout events that, although less frequent, can still occur during the dry season and impact multiple aerosol components simultaneously. The fact that the eBC correlation is higher with the OOA factor than with BBOA (which constitutes only 9 % of PM_{1} , Table 1, Sect. S4) indicates that long-range transport of aged and internally well-mixed biomass burning plumes plays a more important role than nearby sources (Darbyshire et al., 2019). The BBOA factor can be identified by the presence of the m/z 60 and m/z 73 (Fig. 3a), which are dominated by the $\text{C}_2\text{H}_4\text{O}_2^+$ and $\text{C}_3\text{H}_5\text{O}_2^+$ fragments. These fragments originate from levoglucosan and other similar anhydro-sugars (such as mannosan and galactosan). Levoglucosan (1,6- α -D-anhydroglucopyranose, $\text{C}_6\text{H}_{10}\text{O}_5$) is known as a biomarker of biomass burning emissions due to its production from the pyrolysis of carbohydrates as cellulose (Alfarra et al., 2007; Artaxo et al., 2013; Chen et al., 2009; Lee et al., 2010). The signal fraction of m/z 60 for the BBOA factor in our study was 1.5 %, which is 5 times higher than the 0.3 % thresh-

old typically used as an appropriate background fraction for biomass burning (Cubison et al., 2011). OOA presented a m/z 60 signal fraction of 0.2 %, while IEPOX-SOA presented a negligible signal.

The daily profile of BBOA differs significantly from other factors (Fig. 4). While OOA and IEPOX-SOA mass loadings increase during the day, likely due to photochemically driven oxidation processes, BBOA remains relatively constant throughout the day, despite the daytime dilution effect of a rising boundary layer (Andreae et al., 2015). Interestingly, this pattern contrasts with the pronounced daytime decrease in fresh biomass burning aerosol concentrations reported in southwestern Amazonia (Brito et al., 2014), where local fire emissions were more prevalent. The absence of a clear diurnal cycle for BBOA in our study corroborates a regional, rather than local, origin – likely from biomass burning sources located in the eastern Amazon. The flat variability of this primary factor reflects transport over long distances and the influence of complex vertical mixing, including interactions between residual and nocturnal layers (Darbyshire et al., 2019).

Further supporting this hypothesis is the relatively flat daily cycle of eBC, although a slight daytime increase is observed (Fig. 4), possibly due to lensing effects as particles acquire coatings during transport (Denjean et al., 2020). Unlike eBC, NH_4 and NO_3 show minimal diurnal variation, while SO_4 exhibits a daytime increase consistent with secondary production via photochemical reactions from biogenic sources or atmospheric transport processes. The rise in the boundary layer during the afternoon (Fisch et al., 2004) may facilitate the entrainment of particles from above the boundary layer (Darbyshire et al., 2019).

As the OOA and IEPOX-SOA factors together represent around 68 % of the total mass fractions of the submicron particles during our study (Table 1), and, conversely, eBC and BBOA represent only 15 %, the importance of the atmospheric photochemical activity in central Amazonia becomes evident. Well-preserved parts of Amazonia are strongly affected by the regional transport of well-processed biomass burning plumes, overwhelming the local biogenic processes that usually modulate the daily behavior of secondary aerosol development (Artaxo et al., 2013; Darbyshire et al., 2019).

3.2 Physical properties

The mean scattering coefficient at 637 nm in our study was $17 \pm 10 \text{ Mm}^{-1}$ (Table 2), which is similar to the values reported for the same site and at the ATTO site during the dry season in previous years (Rizzo et al., 2013), and lower than observations close to biomass burning sources ($32\text{--}80 \text{ Mm}^{-1}$, Artaxo et al., 2013; Ponczek et al., 2021). In the dry season, fine-mode particles predominate and are more efficient at scattering radiation than coarse-mode-dominated biogenic particles in the wet season (Rizzo et al., 2013). The σ_a mean value was $3 \pm 2 \text{ Mm}^{-1}$ (Table 2, Fig. 5c, Sect. 2.2),

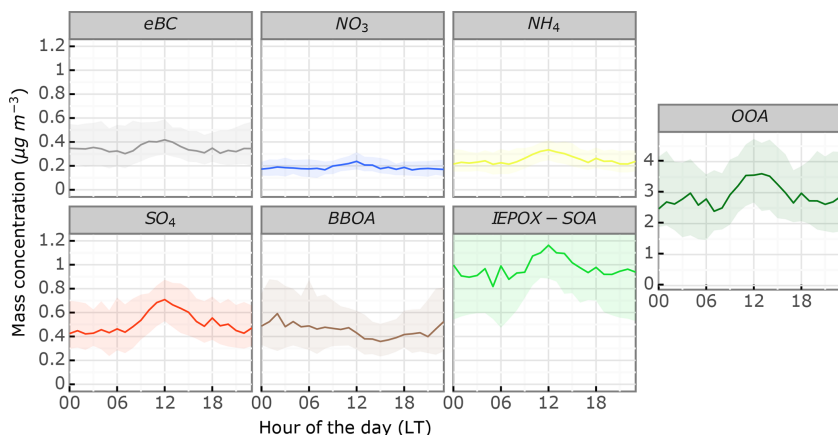


Figure 4. Daily profile (local time) of the PMF derived statistical factors, inorganic chemical species, and eBC mass concentrations for the whole period of measurements (1 August–10 December 2013). The lines represent mean values and the shaded areas represent the standard deviations. The OOA factor, shown separately, has a different vertical scale to improve visualization.

Table 2. Mean and standard deviation of optical properties for the studied period for different wavelengths.

Optical property	Wavelength (nm)	Mean
Scattering coefficient (Mm^{-1})	450	32 ± 19
Scattering coefficient (Mm^{-1})	550	22 ± 13
Scattering coefficient (Mm^{-1})	637	17 ± 10
Scattering coefficient (Mm^{-1})	700	14 ± 8
Absorption coefficient (Mm^{-1})	637	3 ± 2
Single scattering albedo (Mm^{-1})	637	0.87 ± 0.03
Scattering Ångström exponent		1.76 ± 0.26

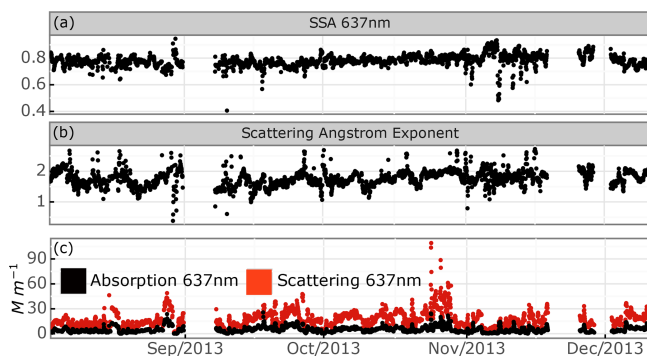


Figure 5. Time series of (a) single scattering albedo (SSA) at 637 nm, (b) the scattering Ångström exponent (SAE), and (c) the absorption and scattering coefficients at 637 nm.

in accordance with the low values previously reported for aged biomass burning haze (Formenti et al., 2003).

The mean SSA observed in our study (0.87 ± 0.03 , Table 2) was very similar to the SSA reported for a nearby site in Amazonia, as well as sites impacted by fires or urban pollution (Carrico et al., 2003; Deng et al., 2016; Kim,

2015; Kleinman et al., 2020; Nakayama et al., 2010; Saturno et al., 2018b; Wang et al., 2017; Zhu et al., 2015). The dominance of organics and the relatively high SO₄ fraction in our study (9 %, Table 1) are probably important factors contributing to the high SSA (Artaxo et al., 2013; Rizzo et al., 2013), and aged biomass burning plumes have been demonstrated to be more efficient in scattering radiation than freshly emitted particles (Formenti et al., 2003). Mean SSA was lower (0.77 ± 0.08 at 637 nm) in a site highly impacted by fires in southwestern Amazonia (Ponczek et al., 2021). In urban environments impacted by pollution, SSA was 0.92–0.89 (Tian et al., 2022), and 0.75–0.84 when the urban pollution was mixed with biomass burning (Pani et al., 2023). Slightly higher SSA values are related to urban haze episodes with high AS contributions, rural areas dominated by dust plumes, or high-altitude regions influenced by clean maritime air masses (Fan et al., 2010; Han et al., 2015; Park et al., 2019). Lower SSA values were influenced by highly absorbing urban pollution (Andreae et al., 2008; Cho et al., 2017; Gao et al., 2015; Jing et al., 2015; Ma et al., 2011; Ram et al., 2016; Soni et al., 2010; Titos et al., 2012) or maritime regions impacted by biomass burning from Africa (Dobrakci et al., 2023). The mean value for the scattering Ångström exponent in our study was 1.76 ± 0.26 (Table 2), which is very similar to the 1.70 ± 0.41 and 1.71 ± 0.24 measured in the dry seasons of previous years at the same site and the nearby ATTO station (Rizzo et al., 2013; Saturno et al., 2018b) and the 1.65 ± 0.37 measured during the dry season at a site more impacted by forest fires (Ponczek et al., 2021). However, it was higher than the 1.48 ± 1.12 (although within the high variability range) and 1.29 ± 0.50 measured in wet seasons of previous years at the same station and the ATTO site (Rizzo et al., 2013; Saturno et al., 2018b). Higher scattering Ångström exponent values are usually related to a greater proportion of fine-mode particles in the aerosol population

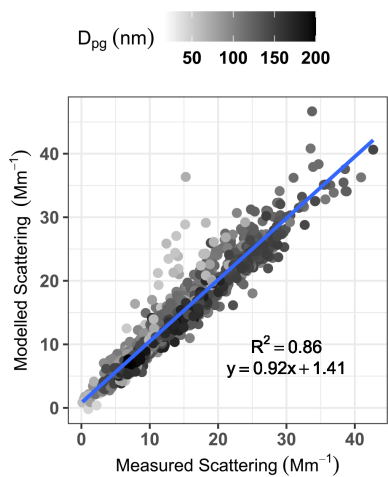


Figure 6. Measured vs. modeled aerosol light scattering at 637 nm. The gray scale corresponds to the equivalent mobility particle diameter for singly charged particles (D_{pg} , Sect. 2.2). The blue line shows the linear regression (slope = 0.92).

(Andreae et al., 2015), and in our case, it is probably related to the occurrence of fresh biomass burning particles.

3.3 Chemical-dependent optical properties

We applied the multiple linear regression (Sect. 2.4.2) to our dataset, and the resulting coefficients successfully predicted the observed scattering ($R^2 = 0.86$, Fig. 6), confirming the validity of this methodology to estimate the specific contribution of each chemical group to the optical properties. We tested the MLR removing AN (due to its low contribution to the PM₁ mass concentration, close to the ACSM detection limit, and therefore, possible artifacts), and the results were comparable, especially for eBC (Table S2). We also tested the robustness of the method by running 100 times MLR on randomly selected 50 % of the data, yielding similar results (Table S3). All standard errors were small (Table 3), and the variance inflation factor was around 3 for IEPOX-SOA, BBOA, AS, and AN, 5.20 for OOA, and 6.19 for eBC. The abovementioned tests suggest that typical MLR caveats such as collinearity had minimal effect on the observed final results. No clear particle size dependency was observed for the radiation scattering in most of the cases (regression fitting under typical conditions of aerosol sizes in the range of 100–150 nm), except at events dominated by ultra-fine particles, at around 50 nm (Fig. 6). This is notably an underestimation of observed scattering at lower particle diameters.

The highest MSE values were attributed to eBC (Table 3, Fig. 7a), followed by the BBOA. Previous studies on plumes dominated by either urban pollution or urban pollution mixed with biomass burning presented MSE values around $4.4 \text{ m}^2 \text{ g}^{-1}$, dominated by organic particles (Cheng et al., 2015; Pani et al., 2023; Tao et al., 2019). The MSE values of the eBC, BBOA, and OOA components calculated

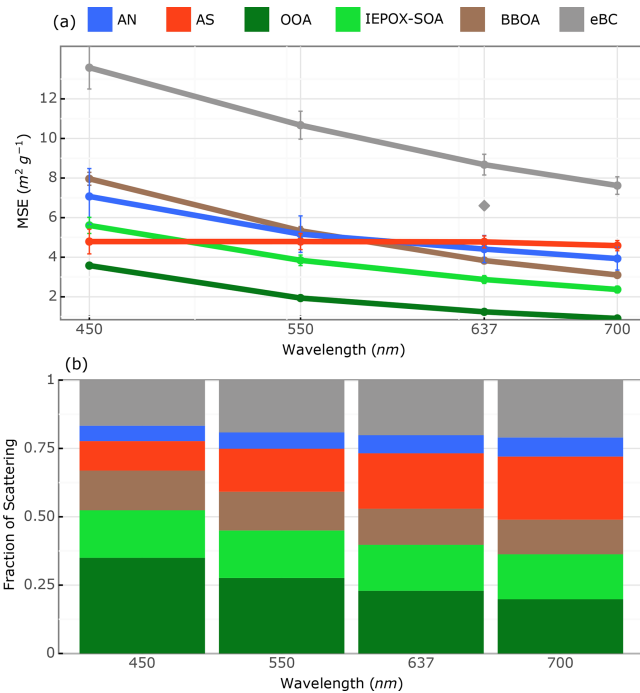


Figure 7. (a) Mass scattering efficiencies of individual chemical components (colored lines) at each wavelength, where the dots are the coefficients obtained from the multilinear regression, with bars indicating the standard errors, and the diamond shape denotes the value of absorption efficiency of eBC at 637 nm; and (b) the fractional contribution of each component to total light scattering.

in our study at 637 nm were circa 180 %, 67 %, and 43 %, respectively, compared to previous measurements in Amazonia, which were highly impacted by biomass burning (Ponczek et al., 2021). The MSE of AS in our study was $4.58\text{--}4.79 \text{ m}^2 \text{ g}^{-1}$ (Table 3, Fig. 7a), in very good agreement with the MSE described for fine-mode ambient AS particles in an urban environment (Tao et al., 2019). Our result is in the lower range of the MSE described in regions impacted by urban pollution ($4.8\text{--}7.1 \text{ m}^2 \text{ g}^{-1}$, Velazquez-Garcia et al., 2023), probably due to the smaller mean diameter found in our study (Fig. 6). However, other regions (urban, remote, rural continental, ocean/marine) presented much smaller MSE values for AS (Cheng et al., 2015; Hand and Malm, 2007). The MSE for AN at 550 nm in our study ($4.79 \text{ m}^2 \text{ g}^{-1}$, Table 3) is in very good agreement with the MSE found in AN in a urban pollution plume (Tao et al., 2019), and within the range previously described in regions highly impacted by urban pollution (Cheng et al., 2015; Tian et al., 2022) and a mixture of urban pollution and biomass burning (Pani et al., 2023).

The organic particles presented higher MSE values for freshly emitted aerosols (BBOA) than for oxygenated particles (OOA) (Table 3), an opposite trend to what was found at PM_{2.5} in a region impacted by urban pollution (Tian et al., 2022). However, previous studies in Amazonia demon-

Table 3. MSE for different wavelengths and aerosol components with standard errors. The variance inflation factor was around 3 for IEPOX-SOA, BBOA, AS and AN, 5.20 for OOA, and 6.19 for eBC, suggesting that typical MLR caveats such as collinearity had minimal effect on the observed final results.

Wavelength (nm)	MSE ($\text{m}^2 \text{ g}^{-1}$)			
	450	550	637	700
eBC	13.58 ± 1.08	10.67 ± 0.70	8.68 ± 0.52	7.62 ± 0.44
BBOA	7.96 ± 0.33	5.33 ± 0.21	3.83 ± 0.16	3.10 ± 0.13
IEPOX-SOA	5.61 ± 0.41	3.84 ± 0.27	2.87 ± 0.20	2.37 ± 0.17
OOA	3.58 ± 0.15	1.94 ± 0.10	1.24 ± 0.07	0.90 ± 0.06
AS	4.79 ± 0.62	4.79 ± 0.41	4.77 ± 0.30	4.58 ± 0.25
AN	7.07 ± 1.41	5.17 ± 0.92	4.41 ± 0.68	3.93 ± 0.58

strated that the size distribution of the particles is mainly below 200 nm, and even aging processes do not appear to cause an overall increase in total particle diameters, probably due to the type of the vegetation, the precursors of SOA, disintegration of larger particles, and other factors (Artaxo et al., 2013; Brito et al., 2014). Fresh biomass burning plumes at 532 nm presented an MSE range of $1.5\text{--}5.7 \text{ m}^2 \text{ g}^{-1}$, depending on the fuel type and plume age (Levin et al., 2010), and the MSE of BBOA found in our study for 550 nm is $5.33 \text{ m}^2 \text{ g}^{-1}$ (Table 3). A review of MSE biomass burning plumes revealed higher MSE values for more aged plumes (Reid et al., 2005). Fine-mode organic aerosols in an urban environment presented a mean MSE of $4.6 \text{ m}^2 \text{ g}^{-1}$ at wavelength 550 nm (Tao et al., 2019), closer to our BBOA MSE (Table 3). The pronounced MSE of the eBC ($7.62\text{--}13.58 \text{ m}^2 \text{ g}^{-1}$, Table 3) is strongly corroborated by other studies that found remarkably high scattering efficiency related to BC, especially when the particles undergo atmospheric processing and aging, as in the case of our study (Bond and Bergstrom, 2006; He et al., 2015; Malm et al., 2005; Pitchford et al., 2007; Romshoo et al., 2021; Schwarz et al., 2006). It has been demonstrated that while aerosol scattering efficiency increases with increasing size, age, and distance from the source, the absorption efficiency remains nearly constant (Kleinman et al., 2020; Zhang et al., 2020). The MSE of elemental carbon in a rural area ranged from $5.4 \text{ m}^2 \text{ g}^{-1}$ to $66.2 \text{ m}^2 \text{ g}^{-1}$, and the high increase was found to be related to sulfate addition during cloud processing (Yu et al., 2010). Recently, with a comparable method, the MSE for eBC has been estimated at $6 \text{ m}^2 \text{ g}^{-1}$ in a site located in western Amazonia. Located within the deforestation arc, the site is strongly impacted by fresh, sometimes local emissions, in contrast to the regional or long-range transport of fires impacting central Amazonia (Ponczek et al., 2021). In regions impacted by urban pollution, the MSE of eBC was $2.6 \text{ m}^2 \text{ g}^{-1}$ (Tao et al., 2019), and it was found not to influence MSE for coarse-mode particles (Titos et al., 2012).

When the mass concentration is considered, the relative contribution of eBC to the scattering in all the measured wavelengths in our study is about 20 %–25 % of the total

scattering (Fig. 7b), comparable to southwestern Amazonia (Ponczek et al., 2021), despite our site having a significantly lower eBC concentration (but higher MSE for eBC). In this same southwestern Amazonia site, the contributions of the OOA and BBOA to MSE were about twice as high as in our study. The contribution of AS and AN to MSE was from 20 % to 30 % with increasing wavelength (Fig. 7b), less than half of that in urban sites in Europe (e.g., 67 % in northern France (Velazquez-Garcia et al., 2023) but about twice as high as during an extreme pollution haze episode (Wang et al., 2015)). As shown in Fig. 7a, the MSE of all components except AS decreases with increasing wavelength, which is consistent with the typical behavior of submicrometric aerosols. This spectral dependence can be attributed to Mie scattering theory, where smaller particles scatter shorter wavelengths more efficiently (Hand and Malm, 2007; Malm et al., 2005). Nonetheless, the variability in the MSE slopes among the different components reflects a complex interplay between aerosol mixing state, refractive index, and size distribution dynamics – particularly the diurnal evolution of each factor's contribution to the total aerosol population (Fig. 4). It is particularly interesting that AS exhibits a distinct spectral behavior typically associated with coarse-mode aerosols, denoting stark differences in its sources and atmospheric processing compared with the other components. Sulfate in Amazonia has been associated with secondary production from biogenic emissions and mixing with primary biogenic organic aerosols (PBOAs) (Martin et al., 2010b; Pöhlker et al., 2012), as well as with coarse-mode particles such as dust and sea salt transported over long distances (Brito et al., 2014; Wu et al., 2019). It is remarkable that the MLR analysis captured this behavior, considering that the ACSM is limited to non-refractory species in the sub-micron range and is not particularly efficient at detecting the sources likely involved. This highlights the sensitivity of the MLR approach to broader aerosol population dynamics, which were captured by the optical instruments operating with a PM_{10} inlet, suggesting the influence of coarse-mode aerosol sources.

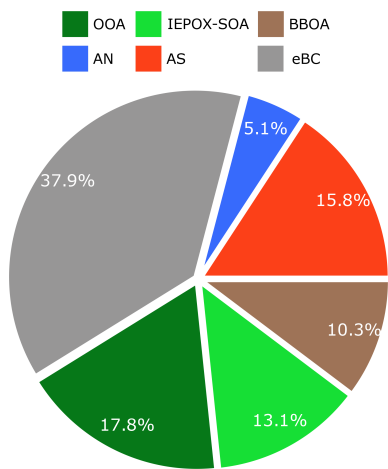


Figure 8. The relative contribution (%) of MEE of each component considering its mass fraction to the total mass of submicrometer particles (Table 1).

While the MSE of eBC does decrease with increasing wavelength (Fig. 7a), its slope (or more precisely, its SAE) is lower than that of other aerosol components. As a result, eBC retains a relatively higher fractional contribution to total scattering at longer wavelengths compared to components with steeper MSE declines (Fig. 7b). The absolute contribution to scattering is determined by both MSE and mass concentration, and although eBC mass concentrations are generally lower, its weaker wavelength dependence allows it to contribute proportionally more at longer wavelengths.

When considering the total light extinction (scattering + absorption), the relative contribution of eBC reaches about 31 % (Fig. 8), which is comparable to the work in a highly urbanized region (Velazquez-Garcia et al., 2023) and an episodic biomass burning event in a rural area (Yu et al., 2010). However, it is less than half of the MEE relative contribution of BC observed during urban pollution episodes (Tian et al., 2022; Yu et al., 2010). The comparison with urban pollution particles' contribution to MEE reveals that the contribution of highly oxygenated particles is very similar (circa 20 %, Fig. 8; Tian et al., 2022), and the most evident difference is the nitrate-based particles, with a much larger contribution in the urban pollution region (Fig. 8; Tian et al., 2022). MEE has been shown to increase by a factor of 3 while freshly emitted smoke from fires ages in the atmosphere, reaching up to $7 \text{ m}^2 \text{ g}^{-1}$ at 532 wavelength (Saide et al., 2022). The OOA factor presented a relatively high contribution to MSE and MEE (Figs. 7b and 8) due to its high fraction of the total PM₁ mass (Table 1), although its MSE is relatively low (Fig. 7a). The contribution of AS to MSE increases with increasing wavelength (from 10 % to 20 %, Fig. 7b), while OOA decreased (from 30 % to 20 %, Fig. 7b).

By using the MSE and MEE ratios, we calculated specific SSA for the eBC, obtaining a value of 0.57. This means that 57 % of the light extinction provoked by the eBC is scattered

rather than absorbed, which is higher than the eBC specific SSA of 0.46 based on previous studies in more polluted conditions (Ponczek et al., 2021; Velazquez-Garcia et al., 2023). The SSA of eBC has been described as typically ranging from 0.3 to 0.4, with higher values associated with heavy coating (Luo et al., 2020), and below 0.3 for pure black carbon (Wang et al., 2021).

A previous study found an eBC absorption cross-section in Amazonia of $12.3 \text{ m}^2 \text{ g}^{-1}$ (Saturno et al., 2018b), and we tested our dataset applying this value (Fig. S14). The result was that eBC mass concentrations decreased by half, with no change in σ_a and SSA, but MSE doubled, while eBC contribution to MEE (Figs. 8, S15) remained unchanged. Due to some methodology differences between our study and Saturno et al. (2018b) (they measured refractory black carbon using a single-particle soot photometer SP2 with a higher cut-off, possibly leading to a sub-estimation of the mass), and the fact that applying the absorption cross-section value they found would make MSE of eBC be an order of magnitude higher than the others (Fig. S14), we opted to remain with the more established value of $6.6 \text{ m}^2 \text{ g}^{-1}$.

4 Conclusions

The results show that the submicrometer particle mass concentration during the dry season ($6.3 \pm 3.3 \mu\text{g m}^{-3}$), which is about an order of magnitude higher than typically observed at this site during the wet season, is highly dominated by the organic fraction ($77 \pm 5 \%$). The organic aerosols were separated into 3 PMF statistical factors, identified as BBOA, OOA, and IEPOX-SOA. The OOA, associated with highly processed and oxidized particles, is the dominant factor ($51 \pm 6 \%$ of the PM₁), followed by IEPOX-SOA (isoprene SOA following a low-NO route, $17 \pm 5 \%$), while the factor more directly associated with fresh biomass burning emissions (BBOA) represents $9 \pm 5 \%$ of PM₁.

The mean radiation scattering coefficient at 637 nm was $17 \pm 10 \text{ Mm}^{-1}$ and the mean absorption coefficient was $3 \pm 2 \text{ Mm}^{-1}$, which is higher than what was observed in the wet season but lower than at sites much more impacted by proximity to fresh forest fires. The SSA of 0.87 ± 0.03 was elevated compared with values previously described in the wet season but was generally in good agreement with SSA values of previous dry seasons – likely an indication of the scattering efficiency of eBC following atmospheric processing and coating. The mean scattering Ångström exponent was 1.76 ± 0.26 , surpassing the values previously measured during the wet season. This is likely due to the greater relative proportion of smaller particles in the aerosol population measured in our study compared with the primary biogenic aerosols, Saharan dust, and sea salt typical of the wet season in central Amazonia.

An MLR analysis of optical properties and different species/factors yielded the highest MSE for eBC in all wave-

lengths ($7.62\text{--}13.58 \text{ m}^2 \text{ g}^{-1}$), followed by the BBOA and AN in the shorter wavelengths (450 and 550 nm) and by AS in the longer wavelengths (637 and 700 nm). Despite having a small mass contribution (6 %), eBC dominated the MEE relative contribution (37.9 %), followed by the OOA (17.8 %). The high MSE of eBC (and a calculated specific SSA of 0.57) is remarkable, and more studies concerning the chemical processing of those particles after their emission are needed in order to understand the processes behind the outstanding efficiency of light scattering of this highly absorbing particle. A special focus should be given to the role of aerosol coating in this process.

Aerosol observations at the heart of Amazonia are extremely challenging. Although our analysis during the dry season yielded robust results, limitations remain – particularly concerning the size distribution of BC and its absorption across multiple wavelengths. To advance our understanding, future studies should prioritize extensive field and laboratory observations aimed at better constraining aerosol coating formation mechanisms and their impact on the radiative scattering properties of BC particles in Amazonia. Increasing the precision of the quantification of the eBC contribution to light scattering has the potential to improve models and reduce uncertainties in global radiative forcing estimations.

Code and data availability. Codes and data are currently available in this link: <https://doi.org/10.5281/zenodo.15345166> (Stern, 2025).

Supplement. The supplement related to this article is available online at <https://doi.org/10.5194/acp-25-9451-2025-supplement>.

Author contributions. RS, JFdB, and PA conceptualized and designed the methodology. RS performed the field measurements, with the support of JFdB. RS, JFdB, SC, LVR, and JDM applied the methodology. RS wrote the original draft, and all the authors discussed the results and commented on the paper.

Competing interests. At least one of the (co-)authors is a member of the editorial board of *Atmospheric Chemistry and Physics*. The peer-review process was guided by an independent editor, and the authors also have no other competing interests to declare.

Disclaimer. Publisher's note: Copernicus Publications remains neutral with regard to jurisdictional claims made in the text, published maps, institutional affiliations, or any other geographical representation in this paper. While Copernicus Publications makes every effort to include appropriate place names, the final responsibility lies with the authors.

Acknowledgements. We thank the Large-scale Biosphere–Atmosphere (LBA) project group and the Clima e Ambiente (CLIAMB) department at Instituto Nacional de Pesquisas da Amazônia (INPA) for continuous support. We thank Alcides Ribeiro, Fernando Morais, Fábio Jorge, Simara Morais for technical and logistics support.

Financial support. This research has been supported by the Natural Environment Research Council (grant no. NE/I030178/1), the Fundação de Amparo à Pesquisa do Estado de São Paulo (grant nos. 2012/14437-9, 2013/05014-0, and 2013/25058-1), the Agence Nationale de la Recherche (grant no. ANR-11-LABX-0005-01), the European Regional Development Fund European Observation Network for Territorial Development and Cohesion (grant no. CA16109), and the Conselho Nacional de Desenvolvimento Científico e Tecnológico (grant no. 304819/2022-0).

Review statement. This paper was edited by Radovan Krejci and reviewed by Weijun Li and one anonymous referee.

References

- Alfarra, M. R., Coe, H., Allan, J. D., Bower, K. N., Boudries, H., Canagaratna, M. R., Jimenez, J. L., Jayne, J. T., Garforth, A. A., Li, S.-M., and Worsnop, D. R.: Characterization of urban and rural organic particulate in the Lower Fraser Valley using two Aerodyne Aerosol Mass Spectrometers, *Atmos. Environ.*, 38, 5745–5758, <https://doi.org/10.1016/j.atmosenv.2004.01.054>, 2004.
- Alfarra, M. R., Prevot, A. S. H., Szidat, S., Sandradewi, J., Weimer, S., Lanz, V. a., Schreiber, D., Mohr, M., and Baltensperger, U.: Identification of the Mass Spectral Signature of Organic Aerosols from Wood Burning Emissions, *Environ. Sci. Technol.*, 41, 5770–5777, <https://doi.org/10.1021/es062289b>, 2007.
- Allan, J. D., Bower, K. N., Coe, H., Boudries, H., Jayne, J. T., Canagaratna, M. R., Millet, D. B., Goldstein, A. H., Quinn, P. K., Weber, R. J., and Worsnop, D. R.: Submicron aerosol composition at Trinidad Head, California, during ITCT 2K2: Its relationship with gas phase volatile organic carbon and assessment of instrument performance, *J. Geophys. Res.-Atmos.*, 109, D23S24, <https://doi.org/10.1029/2003JD004208>, 2004.
- Allan, J. D., Morgan, W. T., Derbyshire, E., Flynn, M. J., Williams, P. I., Oram, D. E., Artaxo, P., Brito, J., Lee, J. D., and Coe, H.: Airborne observations of IEPOX-derived isoprene SOA in the Amazon during SAMBBA, *Atmos. Chem. Phys.*, 14, 11393–11407, <https://doi.org/10.5194/acp-14-11393-2014>, 2014.
- Anderson, T. L. and Ogren, J. A.: Determining Aerosol Radiative Properties Using the TSI 3563 Integrating Nephelometer, *Aerosol Sci. Technol.*, 29, 57–69, <https://doi.org/10.1080/02786829808965551>, 1998.
- Andreae, M. O.: The Biosphere: Pilot or Passenger on Space-ship Earth?, in: *Global Change and Protected Areas*, edited by: Jäger, J. and Aman, H. *Advances in Global Change Research*, vol. 9, Springer, Dordrecht, 59–66, https://doi.org/10.1007/0-306-48051-4_6, 2001.

- Andreae, M. O., Schmid, O., Yang, H., Chand, D., Zhen Yu, J., Zeng, L. M., and Zhang, Y. H.: Optical properties and chemical composition of the atmospheric aerosol in urban Guangzhou, China, *Atmos. Environ.*, 42, 6335–6350, <https://doi.org/10.1016/j.atmosenv.2008.01.030>, 2008.
- Andreae, M. O., Acevedo, O. C., Araújo, A., Artaxo, P., Barbosa, C. G. G., Barbosa, H. M. J., Brito, J., Carbone, S., Chi, X., Cintra, B. B. L., da Silva, N. F., Dias, N. L., Dias-Júnior, C. Q., Ditas, F., Ditz, R., Godoi, A. F. L., Godoi, R. H. M., Heimann, M., Hoffmann, T., Kesselmeier, J., Könenmann, T., Krüger, M. L., Lavric, J. V., Manzi, A. O., Lopes, A. P., Martins, D. L., Mikhailov, E. F., Moran-Zuloaga, D., Nelson, B. W., Nölscher, A. C., Santos Nogueira, D., Piedade, M. T. F., Pöhlker, C., Pöschl, U., Quesada, C. A., Rizzo, L. V., Ro, C.-U., Ruckteschler, N., Sá, L. D. A., de Oliveira Sá, M., Sales, C. B., dos Santos, R. M. N., Saturno, J., Schöngart, J., Sörgel, M., de Souza, C. M., de Souza, R. A. F., Su, H., Targhetta, N., Tóta, J., Trebs, I., Trumbore, S., van Eijck, A., Walter, D., Wang, Z., Weber, B., Williams, J., Winderlich, J., Wittmann, F., Wolff, S., and Yáñez-Serrano, A. M.: The Amazon Tall Tower Observatory (ATTO): overview of pilot measurements on ecosystem ecology, meteorology, trace gases, and aerosols, *Atmos. Chem. Phys.*, 15, 10723–10776, <https://doi.org/10.5194/acp-15-10723-2015>, 2015.
- Araújo, A. C., Nobre, A. D., Kruijt, B., Elbers, A., Dallarosa, R., Stefani, P., von Randow, C., Manzi, A. O., Culf, A. D., Gash, J. H. C., Valentini, R., and Kabat, P.: Comparative measurements of carbon dioxide fluxes from two nearby towers in a central Amazonian rainforest: The Manaus LBA site, *J. Geophys. Res.*, 107, 8090, <https://doi.org/10.1029/2001JD000676>, 2002.
- Artaxo, P., Rizzo, L. V., Brito, J. F., Barbosa, H. M. J., Arana, A., Sena, E. T., Cirino, G. G., Bastos, W., Martin, S. T., and Andreae, M. O.: Atmospheric aerosols in Amazonia and land use change: from natural biogenic to biomass burning conditions, *Faraday Discuss.*, 165, 203–235, <https://doi.org/10.1039/c3fd00052d>, 2013.
- Bond, T. C. and Bergstrom, R. W.: Light absorption by carbonaceous particles: An investigative review, *Aerosol Sci. Technol.*, 40, 27–67, <https://doi.org/10.1080/02786820500421521>, 2006.
- Brito, J., Rizzo, L. V., Morgan, W. T., Coe, H., Johnson, B., Haywood, J., Longo, K., Freitas, S., Andreae, M. O., and Artaxo, P.: Ground-based aerosol characterization during the South American Biomass Burning Analysis (SAMBBA) field experiment, *Atmos. Chem. Phys.*, 14, 12069–12083, <https://doi.org/10.5194/acp-14-12069-2014>, 2014.
- Brito, J., Freney, E., Dominutti, P., Borbon, A., Haslett, S. L., Batenburg, A. M., Colomb, A., Dupuy, R., Denjean, C., Burnet, F., Bourriane, T., Deroubaix, A., Sellegrí, K., Borrman, S., Coe, H., Flamant, C., Knippertz, P., and Schwarzenboeck, A.: Assessing the role of anthropogenic and biogenic sources on PM₁ over southern West Africa using aircraft measurements, *Atmos. Chem. Phys.*, 18, 757–772, <https://doi.org/10.5194/acp-18-757-2018>, 2018.
- Budisulistiorini, S. H., Canagaratna, M. R., Croteau, P. L., Marth, W. J., Baumann, K., Edgerton, E. S., Shaw, S. L., Knipping, E. M., Worsnop, D. R., Jayne, J. T., Gold, A., and Surratt, J. D.: Real-time continuous characterization of secondary organic aerosol derived from isoprene epoxydiols in downtown Atlanta, Georgia, using the aerodyne aerosol chemical speciation monitor, *Environ. Sci. Technol.*, 47, 5686–5694, <https://doi.org/10.1021/es400023n>, 2013.
- Caravan, R. L., Bannan, T. J., Winiberg, F. A. F., Khan, M. A. H., Rousse, A. C., Jasper, A. W., Worrall, S. D., Bacak, A., Artaxo, P., Brito, J., Priestley, M., Allan, J. D., Coe, H., Ju, Y., Osborn, D. L., Hansen, N., Klippenstein, S. J., Shallcross, D. E., Taatjes, C. A., and Percival, C. J.: Observational evidence for Criegee intermediate oligomerization reactions relevant to aerosol formation in the troposphere, *Nat. Geosci.*, 1, 219–226, <https://doi.org/10.1038/s41561-023-01361-6>, 2024.
- Carbone, S., Saarikoski, S., Frey, A., Reyes, F., Reyes, P., Castillo, M., Gramsch, E., Oyola, P., Jayne, J., Worsnop, D. R., and Hillamo, R.: Chemical Characterization of Submicron Aerosol Particles in Santiago de Chile, *Aerosol Air Qual. Res.*, 13, 462–473, <https://doi.org/10.4209/aaqr.2012.10.0261>, 2013.
- Carrico, C. M., Bergin, M. H., Xu, J., Baumann, K., and Marling, H.: Urban aerosol radiative properties: Measurements during the 1999 Atlanta supersite experiment, *J. Geophys. Res.-Atmos.*, 108, 1–17, <https://doi.org/10.1029/2001jd001222>, 2003.
- Chen, G., Canonaco, F., Tobler, A., Aas, W., Alastuey, A., Allan, J., Atabakhsh, S., Aurela, M., Baltensperger, U., Bougiatioti, A., De Brito, J. F., Ceburnis, D., Chazeau, B., Chebaicheb, H., Daellenbach, K. R., Ehn, M., El Haddad, I., Eleftheriadis, K., Favez, O., Flentje, H., Font, A., Fossum, K., Freney, E., Gini, M., Green, D. C., Heikkilä, L., Herrmann, H., Kalogridis, A.-C., Keernik, H., Lhotka, R., Lin, C., Lunder, C., Maasikmets, M., Manousakas, M. I., Marchand, N., Marin, C., Marmureanu, L., Mihalopoulos, N., Močnik, G., Nęcki, J., O'Dowd, C., Ovadnevaite, J., Peter, T., Petit, J.-E., Pikridas, M., Matthew Platt, S., Pokorná, P., Poulain, L., Priestman, M., Riffault, V., Rinaldi, M., Różański, K., Schwarz, J., Sciare, J., Simon, L., Skiba, A., Slowik, J. G., Sosedova, Y., Stavroulas, I., Styszko, K., Teinemaa, E., Timonen, H., Tremper, A., Vasilescu, J., Via, M., Vodička, P., Wiedensohler, A., Zografou, O., Cruz Minguillón, M., and Prévôt, A. S. H.: European aerosol phenomenology – 8: Harmonised source apportionment of organic aerosol using 22 Year-long ACSM/AMS datasets, *Environ. Int.*, 166, 107325, <https://doi.org/10.1016/j.envint.2022.107325>, 2022.
- Chen, Q., Farmer, D. K., Schneider, J., Zorn, S. R., Heald, C. L., Karl, T. G., Guenther, A., Allan, J. D., Robinson, N., Coe, H., Kimmel, J. R., Pauliquevis, T., Borrman, S., Pöschl, U., Andreae, M. O., Artaxo, P., Jimenez, J. L., and Martin, S. T.: Mass spectral characterization of submicron biogenic organic particles in the Amazon Basin, *Geophys. Res. Lett.*, 36, L20806, <https://doi.org/10.1029/2009GL039880>, 2009.
- Chen, Q., Farmer, D. K., Rizzo, L. V., Pauliquevis, T., Kuwata, M., Karl, T. G., Guenther, A., Allan, J. D., Coe, H., Andreae, M. O., Pöschl, U., Jimenez, J. L., Artaxo, P., and Martin, S. T.: Submicron particle mass concentrations and sources in the Amazonian wet season (AMAZE-08), *Atmos. Chem. Phys.*, 15, 3687–3701, <https://doi.org/10.5194/acp-15-3687-2015>, 2015.
- Cheng, Y. F., Wiedensohler, A., Eichler, H., Su, H., Gnauk, T., Brüggemann, E., Herrmann, H., Heintzenberg, J., Slanina, J., Tuch, T., Hu, M., and Zhang, Y. H.: Aerosol optical properties and related chemical apportionment at Xinken in Pearl River Delta of China, *Atmos. Environ.*, 42, 6351–6372, <https://doi.org/10.1016/j.atmosenv.2008.02.034>, 2008.
- Cheng, Z., Jiang, J., Chen, C., Gao, J., Wang, S., Watson, J. G., Wang, H., Deng, J., Wang, B., Zhou, M., Chow, J. C., Pitch-

- ford, M. L., and Hao, J.: Estimation of aerosol mass scattering efficiencies under high mass loading: Case study for the megacity of Shanghai, China, *Environ. Sci. Technol.*, 49, 831–838, <https://doi.org/10.1021/es504567q>, 2015.
- Cho, C., Kim, S.-W., Rupakheti, M., Park, J.-S., Panday, A., Yoon, S.-C., Kim, J.-H., Kim, H., Jeon, H., Sung, M., Kim, B. M., Hong, S. K., Park, R. J., Rupakheti, D., Mahata, K. S., Praveen, P. S., Lawrence, M. G., and Holben, B.: Wintertime aerosol optical and radiative properties in the Kathmandu Valley during the SusKat-ABC field campaign, *Atmos. Chem. Phys.*, 17, 12617–12632, <https://doi.org/10.5194/acp-17-12617-2017>, 2017.
- Cubison, M. J., Ortega, A. M., Hayes, P. L., Farmer, D. K., Day, D., Lechner, M. J., Brune, W. H., Apel, E., Diskin, G. S., Fisher, J. A., Fuelberg, H. E., Hecobian, A., Knapp, D. J., Mikoviny, T., Riemer, D., Sachse, G. W., Sessions, W., Weber, R. J., Weinheimer, A. J., Wisthaler, A., and Jimenez, J. L.: Effects of aging on organic aerosol from open biomass burning smoke in aircraft and laboratory studies, *Atmos. Chem. Phys.*, 11, 12049–12064, <https://doi.org/10.5194/acp-11-12049-2011>, 2011.
- Darbyshire, E., Morgan, W. T., Allan, J. D., Liu, D., Flynn, M. J., Dorsey, J. R., O’Shea, S. J., Lowe, D., Szpek, K., Marenco, F., Johnson, B. T., Bauguitte, S., Haywood, J. M., Brito, J. F., Artaxo, P., Longo, K. M., and Coe, H.: The vertical distribution of biomass burning pollution over tropical South America from aircraft in situ measurements during SAMBBA, *Atmos. Chem. Phys.*, 19, 5771–5790, <https://doi.org/10.5194/acp-19-5771-2019>, 2019.
- Deng, J., Zhang, Y., Hong, Y., Xu, L., Chen, Y., Du, W., and Chen, J.: Optical properties of PM_{2.5} and the impacts of chemical compositions in the coastal city Xiamen in China, *Sci. Total Environ.*, 557–558, 665–675, <https://doi.org/10.1016/j.scitotenv.2016.03.143>, 2016.
- Denjean, C., Brito, J., Libois, Q., Mallet, M., Bourrianne, T., Burnet, F., Dupuy, R., Flamant, C., and Knippertz, P.: Unexpected Biomass Burning Aerosol Absorption Enhancement Explained by Black Carbon Mixing State, *Geophys. Res. Lett.*, 47, 1–11, <https://doi.org/10.1029/2020GL089055>, 2020.
- de Sá, S. S., Palm, B. B., Campuzano-Jost, P., Day, D. A., Newburn, M. K., Hu, W., Isaacman-VanWert, G., Yee, L. D., Thalman, R., Brito, J., Carbone, S., Artaxo, P., Goldstein, A. H., Manzi, A. O., Souza, R. A. F., Mei, F., Shilling, J. E., Springston, S. R., Wang, J., Surratt, J. D., Alexander, M. L., Jimenez, J. L., and Martin, S. T.: Influence of urban pollution on the production of organic particulate matter from isoprene epoxydols in central Amazonia, *Atmos. Chem. Phys.*, 17, 6611–6629, <https://doi.org/10.5194/acp-17-6611-2017>, 2017.
- de Sá, S. S., Rizzo, L. V., Palm, B. B., Campuzano-Jost, P., Day, D. A., Yee, L. D., Wernis, R., Isaacman-VanWert, G., Brito, J., Carbone, S., Liu, Y. J., Sedlacek, A., Springston, S., Goldstein, A. H., Barbosa, H. M. J., Alexander, M. L., Artaxo, P., Jimenez, J. L., and Martin, S. T.: Contributions of biomass-burning, urban, and biogenic emissions to the concentrations and light-absorbing properties of particulate matter in central Amazonia during the dry season, *Atmos. Chem. Phys.*, 19, 7973–8001, <https://doi.org/10.5194/acp-19-7973-2019>, 2019.
- Dobrucki, A., Zuidema, P., Howell, S. G., Saide, P., Freitag, S., Aiken, A. C., Burton, S. P., Sedlacek III, A. J., Redemann, J., and Wood, R.: An attribution of the low single-scattering albedo of biomass burning aerosol over the southeastern Atlantic, *Atmos. Chem. Phys.*, 23, 4775–4799, <https://doi.org/10.5194/acp-23-4775-2023>, 2023.
- Draxler, R. R. and Hess, G. D.: An overview of the HYSPLIT_4 modelling system for trajectories, dispersion and deposition, *Aust. Meteorol. Mag.*, 47, 295–308, 1998.
- Fan, X., Chen, H., Xia, X., Li, Z., and Cribb, M.: Aerosol optical properties from the Atmospheric Radiation Measurement Mobile Facility at Shouxian, China, *J. Geophys. Res.-Atmos.*, 115, D00K33, <https://doi.org/10.1029/2010JD014650>, 2010.
- F. G. Assis, L. F. Ferreira, K. R., Vinhas, L., Maurano, L., Almeida, C., Carvalho, A., Rodrigues, J., Maciel, A., and Camargo, C.: TerraBrasilis: A Spatial Data Analytics Infrastructure for Large-Scale Thematic Mapping, *ISPRS Int. J. Geo-Information*, 8, 513, <https://doi.org/10.3390/ijgi8110513>, 2019.
- Fisch, G., Tota, J., Machado, L. A. T., Silva Dias, M. A. F., da F. Lyra, R. F., Nobre, C. A., Dolman, A. J., and Gash, J. H. C.: The convective boundary layer over pasture and forest in Amazonia, *Theor. Appl. Climatol.*, 78, 47–59, <https://doi.org/10.1007/s00704-004-0043-x>, 2004.
- Flores, B. M., Montoya, E., Sakschewski, B., Nascimento, N., Staal, A., Betts, R. A., Levis, C., Lapola, D. M., Esquivel-Muelbert, A., Jakovac, C., Nobre, C. A., Oliveira, R. S., Borma, L. S., Nian, D., Boers, N., Hecht, S. B., ter Steege, H., Arieira, J., Lucas, I. L., Berenguer, E., Marengo, J. A., Gatti, L. V., Mattos, C. R. C., and Hirota, M.: Critical transitions in the Amazon forest system, *Nature*, 626, 555–564, <https://doi.org/10.1038/s41586-023-06970-0>, 2024.
- Formenti, P., Elbert, W., Maenhaut, W., Haywood, J., Osborne, S., and Andreae, M. O.: Inorganic and carbonaceous aerosols during the Southern African Regional Science Initiative (SAFARI 2000) experiment: Chemical characteristics, physical properties, and emission data or smoke from African biomass burning, *J. Geophys. Res.-Atmos.*, 108, 8488, <https://doi.org/10.1029/2002jd002408>, 2003.
- Forster, P. M., Storelvmo, T., Armour, K., Collins, W., Dufresne, J.-L., Frame, D., Lunt, D. J., Mauritzen, T., Palmer, M. D., Watanabe, M., Wild, M., and Zhang, H.: The Earth’s Energy Budget, Climate Feedbacks and Climate Sensitivity, in: *Climate Change 2021 – The Physical Science Basis. Contribution of Working Group I to the Sixth Assessment Report of the Intergovernmental Panel on Climate Change*, edited by: Masson-Delmotte, V., Zhai, P., Pirani, A., Connors, S. L., Pean, C., Berger, S., Caud, N., and Chen, Y., Cambridge University Press, Cambridge and New York, 923–1054, <https://doi.org/10.1017/9781009157896.009>, 2021.
- Fuzzi, S., Decesari, S., Facchini, M. C., Cavalli, F., Emblico, L., Mircea, M., Andreae, M. O., Trebs, I., Hoffer, A., Guyon, P., Artaxo, P., Rizzo, L. V., Lara, L. L., Pauliquevis, T., Maenhaut, W., Raes, N., Chi, X., Mayol-Bracero, O. L., Soto-García, L. L., Claeys, M., Kourtchev, I., Rissler, J., Swietlicki, E., Tagliavini, E., Schkolnik, G., Falkovich, A. H., Rudich, Y., Fisch, G., and Gatti, L. V.: Overview of the inorganic and organic composition of size-segregated aerosol in Rondônia, Brazil, from the biomass-burning period to the onset of the wet season, *J. Geophys. Res.*, 112, D01201, <https://doi.org/10.1029/2005JD006741>, 2007.
- Gao, Y., Lai, S., Lee, S. C., Yau, P. S., Huang, Y., Cheng, Y., Wang, T., Xu, Z., Yuan, C., and Zhang, Y.: Optical properties of size-resolved particles at a Hong

- Kong urban site during winter, *Atmos. Res.*, 155, 1–12, <https://doi.org/10.1016/j.atmosres.2014.10.020>, 2015.
- Han, T., Qiao, L., Zhou, M., Qu, Y., Du, J., Liu, X., Lou, S., Chen, C., Wang, H., Zhang, F., Yu, Q., and Wu, Q.: Chemical and optical properties of aerosols and their interrelationship in winter in the megacity Shanghai of China, *J. Environ. Sci.*, 27, 59–69, <https://doi.org/10.1016/j.jes.2014.04.018>, 2015.
- Hand, J. L. and Malm, W. C.: Review of aerosol mass scattering efficiencies from ground-based measurements since 1990, *J. Geophys. Res.-Atmos.*, 112, D16203, <https://doi.org/10.1029/2007JD008484>, 2007.
- He, C., Liou, K.-N., Takano, Y., Zhang, R., Levy Zamora, M., Yang, P., Li, Q., and Leung, L. R.: Variation of the radiative properties during black carbon aging: theoretical and experimental intercomparison, *Atmos. Chem. Phys.*, 15, 11967–11980, <https://doi.org/10.5194/acp-15-11967-2015>, 2015.
- Holanda, B. A., Pöhlker, M. L., Walter, D., Saturno, J., Sörgel, M., Ditas, J., Ditas, F., Schulz, C., Franco, M. A., Wang, Q., Donth, T., Artaxo, P., Barbosa, H. M. J., Borrman, S., Braga, R., Brito, J., Cheng, Y., Dollner, M., Kaiser, J. W., Klimach, T., Knote, C., Krüger, O. O., Fütterer, D., Lavrič, J. V., Ma, N., Machado, L. A. T., Ming, J., Morais, F. G., Paulsen, H., Sauer, D., Schlager, H., Schneider, J., Su, H., Weinzierl, B., Walser, A., Wendisch, M., Ziereis, H., Zöger, M., Pöschl, U., Andreae, M. O., and Pöhlker, C.: Influx of African biomass burning aerosol during the Amazonian dry season through layered transatlantic transport of black carbon-rich smoke, *Atmos. Chem. Phys.*, 20, 4757–4785, <https://doi.org/10.5194/acp-20-4757-2020>, 2020.
- Holanda, B. A., Franco, M. A., Walter, D., Artaxo, P., Carbone, S., Cheng, Y., Chowdhury, S., Ditas, F., Gysel-Beer, M., Klimach, T., Kremer, L. A., Krüger, O. O., Lavric, J. V., Lelieveld, J., Ma, C., Machado, L. A. T., Modini, R. L., Morais, F. G., Pozzer, A., Saturno, J., Su, H., Wendisch, M., Wolff, S., Pöhlker, M. L., Andreae, M. O., Pöschl, U., and Pöhlker, C.: African biomass burning affects aerosol cycling over the Amazon, *Commun. Earth Environ.*, 4, 1–15, <https://doi.org/10.1038/s43247-023-00795-5>, 2023.
- Hu, W. W., Campuzano-Jost, P., Palm, B. B., Day, D. A., Ortega, A. M., Hayes, P. L., Krechmer, J. E., Chen, Q., Kuwata, M., Liu, Y. J., de Sá, S. S., McKinney, K., Martin, S. T., Hu, M., Budisulistiorini, S. H., Riva, M., Surratt, J. D., St. Clair, J. M., Isaacman-Van Wertz, G., Yee, L. D., Goldstein, A. H., Carbone, S., Brito, J., Artaxo, P., de Gouw, J. A., Koss, A., Wisthaler, A., Mikoviny, T., Karl, T., Kaser, L., Jud, W., Hansel, A., Docherty, K. S., Alexander, M. L., Robinson, N. H., Coe, H., Allan, J. D., Canagaratna, M. R., Paultot, F., and Jimenez, J. L.: Characterization of a real-time tracer for isoprene epoxydiols-derived secondary organic aerosol (IEPOX-SOA) from aerosol mass spectrometer measurements, *Atmos. Chem. Phys.*, 15, 11807–11833, <https://doi.org/10.5194/acp-15-11807-2015>, 2015.
- Instituto Nacional de Pesquisas Espaciais: Portal do Monitoramento de Queimadas e Incêndios Florestais, Instituto Nacional de Pesquisas Espaciais, http://terrabrasilis.dpi.inpe.br/queimadas/situacao-atual/estatisticas/estatisticas_estados/#afooter (last access: 28 June 2023), 2023.
- Jimenez, J. L., Canagaratna, M. R., Donahue, N. M., Prevot, a. S. H., Zhang, Q., Kroll, J. H., DeCarlo, P. F., Allan, J. D., Coe, H., Ng, N. L., Aiken, a. C., Docherty, K. S., Ulbrich, I. M., Grieshop, A. P., Robinson, A. L., Duplissy, J., Smith, J. D., Wilson, K. R., Lanz, V. A., Hueglin, C., Sun, Y. L., Tian, J., Laaksonen, A., Raatikainen, T., Rautiainen, J., Vaattovaara, P., Ehn, M., Kulmala, M., Tomlinson, J. M., Collins, D. R., Cubison, M. J., Dunlea, J., Huffman, J. A., Onasch, T. B., Alfarra, M. R., Williams, P. I., Bower, K., Kondo, Y., Schneider, J., Drewnick, F., Borrmann, S., Weimer, S., Demerjian, K., Salcedo, D., Cottrell, L., Griffin, R., Takami, A., Miyoshi, T., Hatakeyama, S., Shimono, A., Sun, J. Y., Zhang, Y. M., Dzepina, K., Kimmel, J. R., Sueper, D., Jayne, J. T., Herndon, S. C., Trimborn, A. M., Williams, L. R., Wood, E. C., Middlebrook, A. M., Kolb, C. E., Baltensperger, U., and Worsnop, D. R.: Evolution of Organic Aerosols in the Atmosphere, *Science*, 326, 1525–1529, <https://doi.org/10.1126/science.1180353>, 2009.
- Jing, J., Wu, Y., Tao, J., Che, H., Xia, X., Zhang, X., Yan, P., Zhao, D., and Zhang, L.: Observation and analysis of near-surface atmospheric aerosol optical properties in urban Beijing, *Particuology*, 18, 144–154, <https://doi.org/10.1016/j.partic.2014.03.013>, 2015.
- Kim, K. W.: Optical properties of size-resolved aerosol chemistry and visibility variation observed in the urban site of seoul, korea, *Aerosol Air Qual. Res.*, 15, 271–283, <https://doi.org/10.4209/aaqr.2013.11.0347>, 2015.
- Kleinman, L. I., Sedlacek III, A. J., Adachi, K., Buseck, P. R., Collier, S., Dubey, M. K., Hodshire, A. L., Lewis, E., Onasch, T. B., Pierce, J. R., Shilling, J., Springston, S. R., Wang, J., Zhang, Q., Zhou, S., and Yokelson, R. J.: Rapid evolution of aerosol particles and their optical properties downwind of wildfires in the western US, *Atmos. Chem. Phys.*, 20, 13319–13341, <https://doi.org/10.5194/acp-20-13319-2020>, 2020.
- Kroll, J. H., Ng, N. L., Murphy, S. M., Flagan, R. C., and Seinfeld, J. H.: Secondary Organic Aerosol Formation from Isoprene Photooxidation, *Environ. Sci. Technol.*, 40, 1869–1877, <https://doi.org/10.1021/es0524301>, 2006.
- Laskin, A., Laskin, J., and Nizkorodov, S. A.: Chemistry of Atmospheric Brown Carbon, *Chem. Rev.*, 115, 4335–4382, <https://doi.org/10.1021/cr5006167>, 2015.
- Lee, T., Sullivan, A. P., Mack, L., Jimenez, J. L., Kreidenweis, S. M., Onasch, T. B., Worsnop, D. R., Malm, W., Wold, C. E., Hao, W. M., and Collett, J. L.: Chemical Smoke Marker Emissions During Flaming and Smoldering Phases of Laboratory Open Burning of Wildland Fuels, *Aerosol Sci. Technol.*, 44, <https://doi.org/10.1080/02786826.2010.499884>, 2010.
- Levin, E. J. T., McMeeking, G. R., Carrico, C. M., Mack, L. E., Kreidenweis, S. M., Wold, C. E., Moosmüller, H., Arnott, W. P., Hao, W. M., Collett, J. L., and Malm, W. C.: Biomass burning smoke aerosol properties measured during Fire Laboratory at Missoula Experiments (FLAME), *J. Geophys. Res.-Atmos.*, 115, 1–15, <https://doi.org/10.1029/2009JD013601>, 2010.
- Li, W., Riemer, N., Xu, L., Wang, Y., Adachi, K., Shi, Z., Zhang, D., Zheng, Z., and Laskin, A.: Microphysical properties of atmospheric soot and organic particles: measurements, modeling, and impacts, *npj Clim. Atmos. Sci.*, 7, 65, <https://doi.org/10.1038/s41612-024-00610-8>, 2024.
- Lin, Y. H., Zhang, Z., Docherty, K. S., Zhang, H., Budisulistiorini, S. H., Rubitschun, C. L., Shaw, S. L., Knipping, E. M., Edgerton, E. S., Kleindienst, T. E., Gold, A., and Surratt, J. D.: Isoprene epoxydiols as precursors to secondary organic aerosol formation: Acid-catalyzed reactive uptake studies

- with authentic compounds, *Environ. Sci. Technol.*, 46, 250–258, <https://doi.org/10.1021/es202554c>, 2012.
- Luo, J., Zhang, Y., and Zhang, Q.: The Ångström Exponent and Single-Scattering Albedo of Black Carbon: Effects of Different Coating Materials, *Atmosphere*, 11, 1103, <https://doi.org/10.3390/atmos1101103>, 2020.
- Ma, N., Zhao, C. S., Nowak, A., Müller, T., Pfeifer, S., Cheng, Y. F., Deng, Z. Z., Liu, P. F., Xu, W. Y., Ran, L., Yan, P., Göbel, T., Hallbauer, E., Mildenberger, K., Henning, S., Yu, J., Chen, L. L., Zhou, X. J., Stratmann, F., and Wiedensohler, A.: Aerosol optical properties in the North China Plain during HaChi campaign: an in-situ optical closure study, *Atmos. Chem. Phys.*, 11, 5959–5973, <https://doi.org/10.5194/acp-11-5959-2011>, 2011.
- Malm, W. C., Day, D. E., Carrico, C., Kreidenweis, S. M., Collett, J. L., McMeeking, G., Lee, T., Carrillo, J., and Schichtel, B.: Intercomparison and closure calculations using measurements of aerosol species and optical properties during the Yosemite aerosol characterization study, *J. Geophys. Res.-Atmos.*, 110, 1–21, <https://doi.org/10.1029/2004JD005494>, 2005.
- Marais, E. A., Jacob, D. J., Jimenez, J. L., Campuzano-Jost, P., Day, D. A., Hu, W., Krechmer, J., Zhu, L., Kim, P. S., Miller, C. C., Fisher, J. A., Travis, K., Yu, K., Hanisco, T. F., Wolfe, G. M., Arkinson, H. L., Pye, H. O. T., Froyd, K. D., Liao, J., and McNeill, V. F.: Aqueous-phase mechanism for secondary organic aerosol formation from isoprene: application to the southeast United States and co-benefit of SO₂ emission controls, *Atmos. Chem. Phys.*, 16, 1603–1618, <https://doi.org/10.5194/acp-16-1603-2016>, 2016.
- Martin, S. T., Andreae, M. O., Althausen, D., Artaxo, P., Baars, H., Borrmann, S., Chen, Q., Farmer, D. K., Guenther, A., Gunthe, S. S., Jimenez, J. L., Karl, T., Longo, K., Manzi, A., Müller, T., Pauliquevis, T., Petters, M. D., Prenni, A. J., Pöschl, U., Rizzo, L. V., Schneider, J., Smith, J. N., Swietlicki, E., Tota, J., Wang, J., Wiedensohler, A., and Zorn, S. R.: An overview of the Amazonian Aerosol Characterization Experiment 2008 (AMAZE-08), *Atmos. Chem. Phys.*, 10, 11415–11438, <https://doi.org/10.5194/acp-10-11415-2010>, 2010a.
- Martin, S. T., Andreae, M. O., Artaxo, P., Baumgardner, D., Chen, Q., Goldstein, A. H., Guenther, A., Heald, C. L., Mayol-Bracero, O. L., McMurry, P. H., Pauliquevis, T., Pöschl, U., Prather, K. A., Roberts, G. C., Saleska, S. R., Silva Dias, M. A., Spracklen, D. V., Swietlicki, E., and Trebs, I.: Sources and properties of Amazonian aerosol particles, *Rev. Geophys.*, 48, RG2002, <https://doi.org/10.1029/2008RG000280>, 2010b.
- Martin, S. T., Artaxo, P., Machado, L. A. T., Manzi, A. O., Souza, R. A. F., Schumacher, C., Wang, J., Andreae, M. O., Barbosa, H. M. J., Fan, J., Fisch, G., Goldstein, A. H., Guenther, A., Jimenez, J. L., Pöschl, U., Silva Dias, M. A., Smith, J. N., and Wendisch, M.: Introduction: Observations and Modeling of the Green Ocean Amazon (GoAmazon2014/5), *Atmos. Chem. Phys.*, 16, 4785–4797, <https://doi.org/10.5194/acp-16-4785-2016>, 2016.
- Metcalf, A. R., Loza, C. L., Coggon, M. M., Craven, J. S., Jonsson, H. H., Flagan, R. C., and Seinfeld, J. H.: Secondary organic aerosol coating formation and evaporation: Chamber studies using black carbon seed aerosol and the single-particle soot photometer, *Aerosol Sci. Technol.*, 47, 326–347, <https://doi.org/10.1080/02786826.2012.750712>, 2013.
- Middlebrook, A. M., Bahreini, R., Jimenez, J. L., and Canagaratna, M. R.: Evaluation of Composition-Dependent Collection Efficiencies for the Aerodyne Aerosol Mass Spectrometer using Field Data, *Aerosol Sci. Technol.*, 46, 258–271, <https://doi.org/10.1080/02786826.2011.620041>, 2012.
- Müller, T., Henzing, J. S., de Leeuw, G., Wiedensohler, A., Alastuey, A., Angelov, H., Bizjak, M., Collaud Coen, M., Engström, J. E., Gruening, C., Hillamo, R., Hoffer, A., Imre, K., Ivanov, P., Jennings, G., Sun, J. Y., Kalivitis, N., Karlsson, H., Komppula, M., Laj, P., Li, S.-M., Lunder, C., Marinoni, A., Martins dos Santos, S., Moerman, M., Nowak, A., Ogren, J. A., Petzold, A., Pichon, J. M., Rodriguez, S., Sharma, S., Sheridan, P. J., Teinilä, K., Tuch, T., Viana, M., Virkkula, A., Weingartner, E., Wilhelm, R., and Wang, Y. Q.: Characterization and intercomparison of aerosol absorption photometers: result of two intercomparison workshops, *Atmos. Meas. Tech.*, 4, 245–268, <https://doi.org/10.5194/amt-4-245-2011>, 2011.
- Nah, T., Xu, L., Osborne-Benthaus, K. A., White, S. M., France, S., and Lee Ng, N.: Mixing order of sulfate aerosols and isoprene epoxydiols affects secondary organic aerosol formation in chamber experiments, *Atmos. Environ.*, 217, 116953, <https://doi.org/10.1016/j.atmosenv.2019.116953>, 2019.
- Nakayama, T., Hagino, R., Matsumi, Y., Sakamoto, Y., Kawasaki, M., Yamazaki, A., Uchiyama, A., Kudo, R., Moteki, N., Kondo, Y., and Tonokura, K.: Measurements of aerosol optical properties in central Tokyo during summertime using cavity ring-down spectroscopy: Comparison with conventional techniques, *Atmos. Environ.*, 44, 3034–3042, <https://doi.org/10.1016/j.atmosenv.2010.05.008>, 2010.
- Nascimento, J. P., Bela, M. M., Meller, B. B., Banducci, A. L., Rizzo, L. V., Vara-Vela, A. L., Barbosa, H. M. J., Gomes, H., Rafee, S. A. A., Franco, M. A., Carbone, S., Cirino, G. G., Souza, R. A. F., McKeen, S. A., and Artaxo, P.: Aerosols from anthropogenic and biogenic sources and their interactions – modeling aerosol formation, optical properties, and impacts over the central Amazon basin, *Atmos. Chem. Phys.*, 21, 6755–6779, <https://doi.org/10.5194/acp-21-6755-2021>, 2021.
- Ng, N. L., Herndon, S. C., Trimborn, A., Canagaratna, M. R., Croteau, P. L., Onasch, T. B., Sueper, D., Worsnop, D. R., Zhang, Q., Sun, Y. L., and Jayne, J. T.: An Aerosol Chemical Speciation Monitor (ACSM) for routine monitoring of the composition and mass concentrations of ambient aerosol, *Aerosol Sci. Technol.*, 45, 780–794, <https://doi.org/10.1080/02786826.2011.560211>, 2011.
- Paatero, P. and Tapper, U.: Positive Matrix Factorization: a non-negative factor model with optimal utilization of error estimates of data values, *Environmetrics*, 5, 111–126, 1994.
- Palácios, R. da S., Romera, K. S., Curado, L. F. A., Banga, N. M., Rothmund, L. D., Sallo, F. da S., Morais, D., Santos, A. C. A., Moraes, T. J., Morais, F. G., Landulfo, E., Franco, M. A. de M., Kuhnen, I. A., Marques, J. B., Nogueira, J. d. S., Júnior, L. C. G. D. V., and Rodrigues, T. R.: Long term analysis of optical and radiative properties of aerosols in the amazon basin, *Aerosol Air Qual. Res.*, 20, 139–154, <https://doi.org/10.4209/aaqr.2019.04.0189>, 2020.
- Palm, B. B., de Sá, S. S., Day, D. A., Campuzano-Jost, P., Hu, W., Seco, R., Sjostedt, S. J., Park, J.-H., Guenther, A. B., Kim, S., Brito, J., Wurm, F., Artaxo, P., Thalman, R., Wang, J., Yee, L. D., Wernis, R., Isaacman-VanWertz, G., Goldstein, A. H., Liu, Y., Springston, S. R., Souza, R., Newburn, M. K., Alexander, M. L., Martin, S. T., and Jimenez, J. L.: Secondary or-

- ganic aerosol formation from ambient air in an oxidation flow reactor in central Amazonia, *Atmos. Chem. Phys.*, 18, 467–493, <https://doi.org/10.5194/acp-18-467-2018>, 2018.
- Pani, S. K., Lin, N. H., Wang, S. H., Chantara, S., Griffith, S. M., and Chang, J. H. W.: Aerosol mass scattering efficiencies and single scattering albedo under high mass loading in Chiang Mai valley, Thailand, *Atmos. Environ.*, 308, 119867, <https://doi.org/10.1016/j.atmosenv.2023.119867>, 2023.
- Park, S., Kim, S. W., Lin, N. H., Pani, S. K., Sheridan, P. J., and Andrews, E.: Variability of aerosol optical properties observed at a polluted marine (Gosan, Korea) and a high-altitude mountain (Lulin, Taiwan) site in the Asian continental outflow, *Aerosol Air Qual. Res.*, 19, 1272–1283, <https://doi.org/10.4209/aaqr.2018.11.0416>, 2019.
- Petzold, A., Schloesser, H., Sheridan, P. J., Arnott, W. P., Ogren, J. A., and Virkkula, A.: Evaluation of Multiangle Absorption Photometry for Measuring Aerosol Light Absorption, *Aerosol Sci. Technol.*, 39, 40–51, <https://doi.org/10.1080/027868290901945>, 2005.
- Pitchford, M., Malm, W., Schichtel, B., Kumar, N., Lowenthal, D., and Hand, J.: Revised algorithm for estimating light extinction from IMPROVE particle speciation data, *J. Air Waste Manag. Assoc.*, 57, 1326–1336, <https://doi.org/10.3155/1047-3289.57.11.1326>, 2007.
- Pöhlker, C., Wiedemann, K. T., Sinha, B., Shiraiwa, M., Gunthe, S. S., Smith, M., Su, H., Artaxo, P., Chen, Q., Cheng, Y., Elbert, W., Gilles, M. K., Kilcoyne, A. L. D., Moffet, R. C., Weigand, M., Martin, S. T., Pöschl, U., and Andreae, M. O.: Biogenic Potassium Salt Particles as Seeds for Secondary Organic Aerosol in the Amazon, *Science*, 337, 1075–1078, <https://doi.org/10.1126/science.1223264>, 2012.
- Pöhlker, M. L., Ditas, F., Saturno, J., Klimach, T., Hrabé de Angelis, I., Araújo, A. C., Brito, J., Carbone, S., Cheng, Y., Chi, X., Ditz, R., Gunthe, S. S., Holanda, B. A., Kandler, K., Kesselmeier, J., Könemann, T., Krüger, O. O., Lavrič, J. V., Martin, S. T., Mikhailov, E., Moran-Zuloaga, D., Rizzo, L. V., Rose, D., Su, H., Thalman, R., Walter, D., Wang, J., Wolff, S., Barbosa, H. M. J., Artaxo, P., Andreae, M. O., Pöschl, U., and Pöhlker, C.: Long-term observations of cloud condensation nuclei over the Amazon rain forest – Part 2: Variability and characteristics of biomass burning, long-range transport, and pristine rain forest aerosols, *Atmos. Chem. Phys.*, 18, 10289–10331, <https://doi.org/10.5194/acp-18-10289-2018>, 2018.
- Ponczek, M., Franco, M. A., Carbone, S., Rizzo, L. V., Monteiro dos Santos, D., Morais, F. G., Duarte, A., Barbosa, H. M. J., and Artaxo, P.: Linking the chemical composition and optical properties of biomass burning aerosols in Amazonia, *Environ. Sci. Atmos.*, 2, 252–269, <https://doi.org/10.1039/dlea00055a>, 2021.
- Pöschl, U., Martin, S. T., Sinha, B., Chen, Q., Gunthe, S. S., Huffman, J. A., Borrmann, S., Farmer, D. K., Garland, R. M., Helas, G., Jimenez, J. L., King, S. M., Manzi, A., Mikhailov, E., Pauliquevis, T., Petters, M. D., Prenni, A. J., Roldin, P., Rose, D., Schneider, J., Su, H., Zorn, S. R., Artaxo, P., and Andreae, M. O.: Rainforest Aerosols as Biogenic Nuclei of Clouds and Precipitation in the Amazon, *Science*, 329, 1513–1516, <https://doi.org/10.1126/science.1191056>, 2010.
- Ram, K., Singh, S., Sarin, M. M., Srivastava, A. K., and Tripathi, S. N.: Variability in aerosol optical properties over an urban site, Kanpur, in the Indo-Gangetic Plain: A case study of haze and dust events, *Atmos. Res.*, 174–175, 52–61, <https://doi.org/10.1016/j.atmosres.2016.01.014>, 2016.
- Reid, J. S., Eck, T. F., Christopher, S. A., Koppmann, R., Dubovik, O., Eleuterio, D. P., Holben, B. N., Reid, E. A., and Zhang, J.: A review of biomass burning emissions part III: intensive optical properties of biomass burning particles, *Atmos. Chem. Phys.*, 5, 827–849, <https://doi.org/10.5194/acp-5-827-2005>, 2005.
- Rizzo, L. V., Artaxo, P., Müller, T., Wiedensohler, A., Paixão, M., Cirino, G. G., Arana, A., Swietlicki, E., Roldin, P., Fors, E. O., Wiedemann, K. T., Leal, L. S. M., and Kulmala, M.: Long term measurements of aerosol optical properties at a primary forest site in Amazonia, *Atmos. Chem. Phys.*, 13, 2391–2413, <https://doi.org/10.5194/acp-13-2391-2013>, 2013.
- Romshoo, B., Müller, T., Pfeifer, S., Saturno, J., Nowak, A., Ciupek, K., Quincey, P., and Wiedensohler, A.: Optical properties of coated black carbon aggregates: numerical simulations, radiative forcing estimates, and size-resolved parameterization scheme, *Atmos. Chem. Phys.*, 21, 12989–13010, <https://doi.org/10.5194/acp-21-12989-2021>, 2021.
- Saide, P. E., Thapa, L. H., Ye, X., Pagonis, D., Campuzano-Jost, P., Guo, H., Schuneman, M. L., Jimenez, J. L., Moore, R., Wiggins, E., Winstead, E., Robinson, C., Thornhill, L., Sanchez, K., Wagner, N. L., Ahern, A., Katich, J. M., Perring, A. E., Schwarz, J. P., Lyu, M., Holmes, C. D., Hair, J. W., Fenn, M. A., and Shingler, T. J.: Understanding the Evolution of Smoke Mass Extinction Efficiency Using Field Campaign Measurements, *Geophys. Res. Lett.*, 49, 1–12, <https://doi.org/10.1029/2022GL099175>, 2022.
- Saturno, J., Ditas, F., Penning de Vries, M., Holanda, B. A., Pöhlker, M. L., Carbone, S., Walter, D., Bobrowski, N., Brito, J., Chi, X., Gutmann, A., Hrabe de Angelis, I., Machado, L. A. T., Moran-Zuloaga, D., Rüdiger, J., Schneider, J., Schulz, C., Wang, Q., Wendisch, M., Artaxo, P., Wagner, T., Pöschl, U., Andreae, M. O., and Pöhlker, C.: African volcanic emissions influencing atmospheric aerosols over the Amazon rain forest, *Atmos. Chem. Phys.*, 18, 10391–10405, <https://doi.org/10.5194/acp-18-10391-2018>, 2018a.
- Saturno, J., Holanda, B. A., Pöhlker, C., Ditas, F., Wang, Q., Moran-Zuloaga, D., Brito, J., Carbone, S., Cheng, Y., Chi, X., Ditas, J., Hoffmann, T., Hrabe de Angelis, I., Könemann, T., Lavrič, J. V., Ma, N., Ming, J., Paulsen, H., Pöhlker, M. L., Rizzo, L. V., Schlag, P., Su, H., Walter, D., Wolff, S., Zhang, Y., Artaxo, P., Pöschl, U., and Andreae, M. O.: Black and brown carbon over central Amazonia: long-term aerosol measurements at the ATTO site, *Atmos. Chem. Phys.*, 18, 12817–12843, <https://doi.org/10.5194/acp-18-12817-2018>, 2018b.
- Schuster, G. L., Dubovik, O., and Holben, B. N.: Angstrom exponent and bimodal aerosol size distributions, *J. Geophys. Res.-Atmos.*, 111, D07207, <https://doi.org/10.1029/2005JD006328>, 2006.
- Schwarz, J. P., Gao, R. S., Fahey, D. W., Thomson, D. S., Watts, L. A., Wilson, J. C., Reeves, J. M., Darbeheshti, M., Baumgardner, D. G., Kok, G. L., Chung, S. H., Schulz, M., Hendricks, J., Lauer, A., Kärcher, B., Slowik, J. G., Rosenlof, K. H., Thompson, T. L., Langford, A. O., Loewenstein, M., and Aikin, K. C.: Single-particle measurements of midlatitude black carbon and light-scattering aerosols from the boundary layer to the lower stratosphere, *J. Geophys. Res.-Atmos.*, 111, 1–15, <https://doi.org/10.1029/2006JD007076>, 2006.

- Sena, E. T., Artaxo, P., and Correia, A. L.: Spatial variability of the direct radiative forcing of biomass burning aerosols and the effects of land use change in Amazonia, *Atmos. Chem. Phys.*, 13, 1261–1275, <https://doi.org/10.5194/acp-13-1261-2013>, 2013.
- Shrivastava, M., Andreae, M. O., Artaxo, P., Barbosa, H. M. J., Berg, L. K., Brito, J., Ching, J., Easter, R. C., Fan, J., Fast, J. D., Feng, Z., Fuentes, J. D., Glasius, M., Goldstein, A. H., Alves, E. G., Gomes, H., Gu, D., Guenther, A., Jathar, S. H., Kim, S., Liu, Y., Lou, S., Martin, S. T., McNeill, V. F., Medeiros, A., de Sá, S. S., Shilling, J. E., Springston, S. R., Souza, R. A. F., Thornton, J. A., Isaacman-VanWertz, G., Yee, L. D., Ynoue, R., Zaveri, R. A., Zelenyuk, A., and Zhao, C.: Urban pollution greatly enhances formation of natural aerosols over the Amazon rainforest, *Nat. Commun.*, 10, 1046, <https://doi.org/10.1038/s41467-019-08909-4>, 2019.
- Soni, K., Singh, S., Bano, T., Tanwar, R. S., Nath, S., and Arya, B. C.: Variations in single scattering albedo and Angstrom absorption exponent during different seasons at Delhi, India, *Atmos. Environ.*, 44, 4355–4363, <https://doi.org/10.1016/j.atmosenv.2010.07.058>, 2010.
- Stern, R. and Müller, J.: Dataset and code for article: "Strong influence of Black Carbon on aerosol optical properties in Central Amazonia during the fire season" published at ACP, in: *Atmospheric Chemistry and Physics*, Zenodo [data set], <https://doi.org/10.5281/zenodo.15345166>, 2025.
- Sun, J., Zhang, Q., Canagaratna, M. R., Zhang, Y., Ng, N. L., Sun, Y., Jayne, J. T., Zhang, X., Zhang, X., and Worsnop, D. R.: Highly time- and size-resolved characterization of submicron aerosol particles in Beijing using an Aerodyne Aerosol Mass Spectrometer, *Atmos. Environ.*, 44, 131–140, <https://doi.org/10.1016/j.atmosenv.2009.03.020>, 2010.
- Surratt, J. D., Chan, A. W. H., Eddingsaas, N. C., Chan, M., Loza, C. L., Kwan, A. J., Hersey, S. P., Flagan, R. C., Wennberg, P. O., and Seinfeld, J. H.: Reactive intermediates revealed in secondary organic aerosol formation from isoprene, *P. Natl. Acad. Sci. USA*, 107, 6640–6645, <https://doi.org/10.1073/pnas.0911114107>, 2010.
- Szopa, S., Naik, V., Artaxo, P., Berntsen, T., Collins, W. D., Fuzzi, S., Gallardo, L., Kiendler-Scharr, A., Klimont, Z., Liao, H., Unger, N., and Zanis, P.: Short-lived Climate Forcers, in: *Climate Change 2021 – The Physical Science Basis*, edited by: Masson-Delmotte, V., Zhai, P., Pirani, A., Connors, S. L., Péan, C., Berger, S., Caud, N., Chen, Y., Goldfarb, L., Gomis, M. I., Huang, M., Leitzell, K., Lonnoy, E., Matthews, J. B. R., Maycock, T. K., Waterfield, T., Yelekçi, O., Yu, R., and Zhou, B., Cambridge University Press, 817–922, <https://doi.org/10.1017/9781009157896.007>, 2023. Masson-Delmotte, V., Zhai, P., Pirani, A., Connors, S. L., Péan, C., Berger, S., Caud, N., Chen, Y., Goldfarb, L., Gomis, M. I., Huang, M., Leitzell, K., Lonnoy, E., Matthews, J. B. R., Maycock, T. K., Waterfield, T., Yelekçi, O., Yu, R., and Zhou, B., Cambridge University Press, Cambridge, United Kingdom and New York, NY, USA, pp. 817–922, <https://doi.org/10.1017/9781009157896.007>, 2021.
- Tao, J., Zhang, Z., Wu, Y., Zhang, L., Wu, Z., Cheng, P., Li, M., Chen, L., Zhang, R., and Cao, J.: Impact of particle number and mass size distributions of major chemical components on particle mass scattering efficiency in urban Guangzhou in southern China, *Atmos. Chem. Phys.*, 19, 8471–8490, <https://doi.org/10.5194/acp-19-8471-2019>, 2019.
- Tasoglou, A., Saliba, G., Subramanian, R., and Pandis, S. N.: Absorption of chemically aged biomass burning carbonaceous aerosol, *J. Aerosol Sci.*, 113, 141–152, <https://doi.org/10.1016/j.jaerosci.2017.07.011>, 2017.
- Tian, J., Wang, Q., Liu, H., Ma, Y., Liu, S., Zhang, Y., Ran, W., Han, Y., and Cao, J.: Measurement report: The importance of biomass burning in light extinction and direct radiative effect of urban aerosol during the COVID-19 lockdown in Xi'an, China, *Atmos. Chem. Phys.*, 22, 8369–8384, <https://doi.org/10.5194/acp-22-8369-2022>, 2022.
- Titos, G., Foyo-Moreno, I., Lyamani, H., Querol, X., Alastuey, A., and Alados-Arboledas, L.: Optical properties and chemical composition of aerosol particles at an urban location: An estimation of the aerosol mass scattering and absorption efficiencies, *J. Geophys. Res.-Atmos.*, 117, 1–12, <https://doi.org/10.1029/2011JD016671>, 2012.
- Tuch, T. M., Haudek, A., Müller, T., Nowak, A., Wex, H., and Wiedensohler, A.: Design and performance of an automatic regenerating adsorption aerosol dryer for continuous operation at monitoring sites, *Atmos. Meas. Tech.*, 2, 417–422, <https://doi.org/10.5194/amt-2-417-2009>, 2009.
- Ulbrich, I. M., Canagaratna, M. R., Zhang, Q., Worsnop, D. R., and Jimenez, J. L.: Interpretation of organic components from Positive Matrix Factorization of aerosol mass spectrometric data, *Atmos. Chem. Phys.*, 9, 2891–2918, <https://doi.org/10.5194/acp-9-2891-2009>, 2009.
- Velazquez-Garcia, A., Crumeyrolle, S., de Brito, J. F., Tison, E., Bourrianne, E., Chiappello, I., and Riffault, V.: Deriving composition-dependent aerosol absorption, scattering and extinction mass efficiencies from multi-annual high time resolution observations in Northern France, *Atmos. Environ.*, 298, 119613, <https://doi.org/10.1016/j.atmosenv.2023.119613>, 2023.
- Virtanen, P., Gommers, R., Oliphant, T. E., Haberland, M., Reddy, T., Cournapeau, D., Burovski, E., Peterson, P., Weckesser, W., Bright, J., van der Walt, S. J., Brett, M., Wilson, J., Millman, K. J., Mayorov, N., Nelson, A. R. J., Jones, E., Kern, R., Larson, E., Carey, C. J., Polat, I., Feng, Y., Moore, E. W., VanderPlas, J., Laxalde, D., Perktold, J., Cimrman, R., Henriksen, I., Quintero, E. A., Harris, C. R., Archibald, A. M., Ribeiro, A. H., Pedregosa, F., van Mulbregt, P., Vijaykumar, A., Bardelli, A. P., Rothberg, A., Hilboll, A., Kloeckner, A., Scopatz, A., Lee, A., Rokem, A., Woods, C. N., Fulton, C., Masson, C., Häggström, C., Fitzgerald, C., Nicholson, D. A., Hagen, D. R., Pasechnik, D. V., Olivetti, E., Martin, E., Wieser, E., Silva, F., Lenders, F., Wilhelm, F., Young, G., Price, G. A., Ingold, G.-L., Allen, G. E., Lee, G. R., Audren, H., Probst, I., Dietrich, J. P., Silterra, J., Webber, J. T., Slavić, J., Nothman, J., Buchner, J., Kulick, J., Schönberger, J. L., de Miranda Cardoso, J. V., Reimer, J., Harrington, J., Rodríguez, J. L. C., Nunez-Iglesias, J., Kuczynski, J., Tritz, K., Thoma, M., Newville, M., Kümmeler, M., Bolingbroke, M., Tartre, M., Pak, M., Smith, N. J., Nowaczyk, N., Shebanov, N., Pavlyk, O., Brodtkorb, P. A., Lee, P., McGibbon, R. T., Feldbauer, R., Lewis, S., Tygier, S., Sievert, S., Vigna, S., Peterson, S., More, S., Pudlik, T., Oshima, T., Pingel, T. J., Robitaille, T. P., Spura, T., Jones, T. R., Cera, T., Leslie, T., Zito, T., Krauss, T., Upadhyay, U., Halchenko, Y. O., Vázquez-Baeza, Y., and SciPy 1.0 Contributors: SciPy 1.0: fundamental algorithms

- for scientific computing in Python, *Nat. Methods*, 17, 261–272, <https://doi.org/10.1038/s41592-019-0686-2>, 2020.
- Wang, H., Shi, G., Tian, M., Zhang, L., Chen, Y., Yang, F., and Cao, X.: Aerosol optical properties and chemical composition apportionment in Sichuan Basin, China, *Sci. Total Environ.*, 577, 245–257, <https://doi.org/10.1016/j.scitotenv.2016.10.173>, 2017.
- Wang, Q., Sun, Y., Jiang, Q., Du, W., Sun, C., Fu, P., and Wang, Z.: Chemical composition of aerosol particles and light extinction apportionment before and during the heating season in Beijing, China, *J. Geophys. Res.-Atmos.*, 120, 12708–12722, <https://doi.org/10.1002/2015JD023871>, 2015.
- Wang, Q., Saturno, J., Chi, X., Walter, D., Lavric, J. V., Moran-Zuloaga, D., Ditas, F., Pöhlker, C., Brito, J., Carbonne, S., Artaxo, P., and Andreae, M. O.: Modeling investigation of light-absorbing aerosols in the Amazon Basin during the wet season, *Atmos. Chem. Phys.*, 16, 14775–14794, <https://doi.org/10.5194/acp-16-14775-2016>, 2016.
- Wang, Y., Pang, Y., Huang, J., Bi, L., Che, H., Zhang, X., and Li, W.: Constructing Shapes and Mixing Structures of Black Carbon Particles With Applications to Optical Calculations, *J. Geophys. Res.-Atmos.*, 126, 1–15, <https://doi.org/10.1029/2021JD034620>, 2021.
- Wennberg, P. O., Bates, K. H., Crounse, J. D., Dodson, L. G., McVay, R. C., Mertens, L. A., Nguyen, T. B., Praske, E., Schwantes, R. H., Smarte, M. D., St Clair, J. M., Teng, A. P., Zhang, X., and Seinfeld, J. H.: Gas-Phase Reactions of Isoprene and Its Major Oxidation Products, *Chem. Rev.*, 118, 3337–3390, <https://doi.org/10.1021/acs.chemrev.7b00439>, 2018.
- Whitehead, J. D., Derbyshire, E., Brito, J., Barbosa, H. M. J., Crawford, I., Stern, R., Gallagher, M. W., Kaye, P. H., Allan, J. D., Coe, H., Artaxo, P., and McFiggans, G.: Biogenic cloud nuclei in the central Amazon during the transition from wet to dry season, *Atmos. Chem. Phys.*, 16, 9727–9743, <https://doi.org/10.5194/acp-16-9727-2016>, 2016.
- Wiedensohler, A., Birmili, W., Nowak, A., Sonntag, A., Weinhold, K., Merkel, M., Wehner, B., Tuch, T., Pfeifer, S., Fiebig, M., Fjäraa, A. M., Asmi, E., Sellegri, K., Depuy, R., Venzac, H., Villani, P., Laj, P., Aalto, P., Ogren, J. A., Swietlicki, E., Williams, P., Roldin, P., Quincey, P., Hüglin, C., Fierz-Schmidhauser, R., Gysel, M., Weingartner, E., Riccobono, F., Santos, S., Grünig, C., Faloon, K., Beddows, D., Harrison, R., Monahan, C., Jennings, S. G., O'Dowd, C. D., Marinoni, A., Horn, H.-G., Keck, L., Jiang, J., Scheckman, J., McMurry, P. H., Deng, Z., Zhao, C. S., Moerman, M., Henzing, B., de Leeuw, G., Löschau, G., and Bastian, S.: Mobility particle size spectrometers: harmonization of technical standards and data structure to facilitate high quality long-term observations of atmospheric particle number size distributions, *Atmos. Meas. Tech.*, 5, 657–685, <https://doi.org/10.5194/amt-5-657-2012>, 2012.
- Wu, L., Li, X., Kim, H., Geng, H., Godoi, R. H. M., Barbosa, C. G. G., Godoi, A. F. L., Yamamoto, C. I., de Souza, R. A. F., Pöhlker, C., Andreae, M. O., and Ro, C.-U.: Single-particle characterization of aerosols collected at a remote site in the Amazonian rainforest and an urban site in Manaus, Brazil, *Atmos. Chem. Phys.*, 19, 1221–1240, <https://doi.org/10.5194/acp-19-1221-2019>, 2019.
- Xu, L., Guo, H., Boyd, C. M., Klein, M., Bougiatioti, A., Cerully, K. M., Hite, J. R., Isaacman-VanWertz, G., Kreisberg, N. M., Knote, C., Olson, K., Koss, A., Goldstein, A. H., Hering, S. V., de Gouw, J., Baumann, K., Lee, S.-H., Nenes, A., Weber, R. J., and Ng, N. L.: Effects of anthropogenic emissions on aerosol formation from isoprene and monoterpenes in the southeastern United States, *P. Natl. Acad. Sci. USA*, 112, 37–42, <https://doi.org/10.1073/pnas.1417609112>, 2015.
- Yamasoe, H. A., Artaxo, P., Miguel, A. H., and Allen, A. G.: Chemical composition of aerosol particles from direct emissions of vegetation fires in the Amazon Basin: water-soluble species and trace elements, *Atmos. Environ.*, 34, 1641–1653, [https://doi.org/10.1016/S1352-2310\(99\)00329-5](https://doi.org/10.1016/S1352-2310(99)00329-5), 2000.
- Yáñez-Serrano, A. M., Nölscher, A. C., Williams, J., Wolff, S., Alves, E., Martins, G. A., Bourtsoukidis, E., Brito, J., Jardine, K., Artaxo, P., and Kesselmeier, J.: Diel and seasonal changes of biogenic volatile organic compounds within and above an Amazonian rainforest, *Atmos. Chem. Phys.*, 15, 3359–3378, <https://doi.org/10.5194/acp-15-3359-2015>, 2015.
- Yu, H., Wu, C., Wu, D., and Yu, J. Z.: Size distributions of elemental carbon and its contribution to light extinction in urban and rural locations in the pearl river delta region, China, *Atmos. Chem. Phys.*, 10, 5107–5119, <https://doi.org/10.5194/acp-10-5107-2010>, 2010.
- Zaveri, R. A., Wang, J., Fan, J., Zhang, Y., Shilling, J. E., Zelenyuk, A., Mei, F., Newsom, R., Pekour, M., Tomlinson, J., Comstock, J. M., Shrivastava, M., Fortner, E., Machado, L. A. T., Artaxo, P., and Martin, S. T.: Rapid growth of anthropogenic organic nanoparticles greatly alters cloud life cycle in the Amazon rainforest, *Sci. Adv.*, 8, 1–17, <https://doi.org/10.1126/sciadv.abj0329>, 2022.
- Zhang, Q., Jimenez, J. L., Canagaratna, M. R., Ulbrich, I. M., Ng, N. L., Worsnop, D. R., and Sun, Y.: Understanding atmospheric organic aerosols via factor analysis of aerosol mass spectrometry: A review, *Anal. Bioanal. Chem.*, 401, 3045–3067, <https://doi.org/10.1007/s00216-011-5355-y>, 2011.
- Zhang, Y., Zhi, G., Jin, W., Wang, L., Guo, S., Shi, R., Sun, J., Cheng, M., Bi, F., Gao, J., Zhang, B., Wu, J., Shi, Z., Liu, B., Wang, Z., and Li, S.: Differing effects of escalating pollution on absorption and scattering efficiencies of aerosols: Toward co-beneficial air quality enhancement and climate protection measures, *Atmos. Environ.*, 232, 117570, <https://doi.org/10.1016/j.atmosenv.2020.117570>, 2020.
- Zhu, C. S., Cao, J. J., Ho, K. F., Antony Chen, L. W., Huang, R. J., Wang, Y. C., Li, H., Shen, Z. X., Chow, J. C., Watson, J. G., Su, X.-L., Wang, Q.-Y. and Xiao, S.: The optical properties of urban aerosol in northern China: A case study at Xi'an, *Atmos. Res.*, 160, 59–67, <https://doi.org/10.1016/j.atmosres.2015.03.008>, 2015.